



Escola Tècnica Superior d'Enginyeria
de Telecomunicació de Barcelona

UNIVERSITAT POLITÈCNICA DE CATALUNYA

PROJECTE FINAL DE CARRERA

Monitorització d'incendis amb imatges desde satel·lit i amb UAV

(Fire monitoring with satellite and UAV
imagery)

Estudis: Enginyeria de Electrònica

Autor: Carles Lloret Salvo

Director/a: Mercè M. Vall-Ilossera Ferran

Any: primavera 2015-2016

Abstract

Wildfires are of major concern now days because, even though they have also a natural role, they have negative impacts in environmental, economic and social terms. The main purposes of this project are the study, combination, comparison of different ways to sense fires. It focus on the images and data -that remotely sensed by instruments- provided and transmitted from satellites and drones. Its uttermost purpose is to design ways to detect, trace, measure the burned areas from UAV and give a comprehensive view of the wildfire while it is taking place. It deepens into the nature of forest fires and relates how factors like wind or terrain affect their propagation and growth. In the case of UAV, based on the information received from the sensors at an altitude between 10km and 20km, the project discusses how to measure the burned areas. Despite there is little data or imagery recorded with specific instruments from this altitude while a forest fire is taking place at this stage, it is enough to draw some lines of action. Meanwhile, satellite images and data of forest fires already occurred are easily available, we had no forest fires images recorded by UAVs or other airplanes at 10 or 20km height. Consequently, many algorithm of detection and monitoring using only images from satellite (both when there is no fire and when there is burning a fire) and images from sensors flying on UAVs.. With all that information regarding the sensors and the patterns of the fire it is possible to discern the movements of the fire. Once the movements and growth are recorded and known, a drone-based easy-to-understand chart of the wildfire is delivered.

Los incendios constituyen una gran preocupación hoy en dia, a pesar que a veces juegan un papel natural, también tienen un impacto negativo en términos medioambientales, económicos y sociales. Este proyecto consiste en el estudio , la combinación , la comparación de diferentes maneras para detectar, medir y entender los incendios. Se centra en el estudio de las imágenes y datos captados remotamente por sensores -y camaras- desde satélite y desde aviones no tripulados. Su máximo objetivo es diseñar maneras de detectar , rastrear , medir las áreas quemadas y dar una visión comprehensiva de un incendio forestal mientras este tiene lugar. Se profundiza en la naturaleza del fuego durante los incendios forestales y como factores como el viento o el terreno afecta su propagación y crecimiento. Basándose en información recibida desde sensores a una altitud de entre 10km y 20km, el proyecto discute como medir la áreas quemadas. A pesar que no hay muchos datos o imágenes de incendios grabados desde drones a esta altitud con ciertos instrumentos mientras este ocurre, eso es suficiente para plantear unas lineas de estudio y trabajo. Con las características de ciertos sensores y los patrones descritos por el fuego es posible discernir los movimientos del

incendio. Una vez grabados y conocidos tales movimientos debería ser posible mostrar un mapa o diagrama del incendio fácil de entender basado en drones para la gente que esta sobre el terreno.

Els focs forestals constitueixen una gran preocupació avui en dia, malgrat que a vegades juguen un paper natural, també tenen un impacte negatiu en termes ambientals, econòmics y socials. Aquest projecte consisteix en l'estudi, la combinació , la comparació de diferents maneres per detectar incendis. Es centra en el estudi de imatges i dades produïdes i transmeses per sensors desde satel·lits i per avions no tripulats. El seu màxim objectiu és dissenyar maneres de detectar , rastrejar , mesurar les àrees cremades y donar una visió comprensiva d'in incendi forestal mentre aquest es produeix. S'aprofundeix en la naturalesa del foc durant els incendis forestals i com factors com el vent o el terreny afecten la seva propagació i creixement. En el cas dels UAV o drones, basant-se en la informació rebuda des dels sensors a una altitud d'entre 10km i 20km, el projecte discuteix com mesurar les arees cremades. Malgrat que no existeix moltes dades o imatges sobre incendis a aquestes altituds grabades per drones, es suficient per plantejar unes lines d'estudi, treball i acció. Amb les característiques del sensors i els patrons descrits pel foc seria possible discernir els moviments del incendi. Llavors un cop grabats i coneguts aquest creixement hauria de ser possible mostrar un mapa o diagrames útils i fàcils d'entendre basat en drones per a la gent que esta sobre el terreny.

Acknowledgments

I would like to express my gratitude towards my supervisor Mercè M. Vall-llossera Ferran who guided this project despite sometimes I was lost in the search and amount of information and data available. I usually had a lot of information and many paths to investigate. Without her and other professors I would be lost. I am also happy to be able to investigate and research topics like drones and climate-related satellite data analysis. Fortunately -or not-, through this tasks I obtained information about forest fires near places I live.

I would like to point out the openness and easiness provided by the EUMETSAT too. I thank the EUMETSAT for all their free information they upload online which make possible to accomplish and even improve this work. I asked them for the data and imagery they provided tirelessly. It is fortunate that the EUMETSAT staff provides a large volume of satellite imagery and information for free with a small delay. I have also requested a large amount of information for mere curiosity without any cost and easily.

My most inner thoughts go to my parents and my brother who suffered my crazy time tables and some absences when I was required especially during the summer. I frustrated some familiar reunions. I hope some day I will be able to repay all my debt with them somehow. Nonetheless, they believe in me and my efforts.

Index of Contents

1.Introduction	10
1.1.Mission.....	12
1.2.Scope.....	12
1.3.Hypothesis	12
2.Study of the different analysis.....	14
2.1.Tools for forest fire prevention detection and monitoring.....	14
2.2.Space-borne analysis.....	15
2.2.1. Radar analysis.....	15
2.2.2.Space-borne radiometric analysis	16
2.2.3. SEVIRI.....	20
2.2.4. Fire detection algorithms.....	27
2.2.5. Thresholding contextual algorithms.....	27
2.2.6. Thresholding multi-temporal algorithms.....	29
2.2.7. Study Case and Data samples : Forest fires in North Catalonia.....	31
2.2.8.Thresholding Contextual algorithms applied.....	48
2.2.9. Thresholding Multi-temporal algorithms applied.....	52
2.3.UAV Analysis.....	57
2.3.1.Understanding the stages of the proposed UAV deployments.....	57
2.3.2. Unmanned Air Vehicle.....	61
2.3.3. UAV imagery errors and distortions:.....	62
2.3.4. Payload Cameras:.....	64
2.4.Study of the wildfire.....	70
2.4.1.The shape of fire.....	72
2.4.2.Color of fire.....	77
2.4.3. UAV cost.....	83
2.5.Manned aircraft-borne analysis.	84
2.6.Fire lookout towers.....	84
2.6.1. Forest watch towers cost.....	85
3.Recognition and analysis of forest fire from one or more drones.....	87
4.Epilogue.....	90
4.1.Comparisons and costs.....	90
4.2.Conclusions.....	90
4.3.Recommendations for further research	91
5.References.....	91
6.Bibliography.....	92

Illustration Index

Illustration 2.2.1.1: Backscatter depending on the fire.....	15
Illustration 2.2.2.1: Black body radiation and the visible spectrum.....	16
Illustration 2.2.2.2 Relation between black body radiation and brightness temperature.....	18
Illustration 2.2.3.1: Atmospheric absorption for different wavelength.....	22
Illustration 2.2.3.2: Wavelengths not affected by atmospheric absorption nor scattering.....	23
Illustration 2.2.3.3: Scheme of the SEVIRI radiometer.....	24
Illustration 2.2.3.4: West-East level 1.5 ground resolution.....	25
Illustration 2.2.3.5: North-South level 1.5 ground resolution.....	25
Illustration 2.2.5.1: Thresholding contextual algorithms sweeping process.....	28
Illustration 2.2.6.1: Temperature from a pixel that suffers the fire anomaly.....	31
Illustration 2.2.7.1: Precise burned area by the fire.....	32
Illustration 2.2.7.2: Longitude and latitude of LaJonquera fire.....	33
Illustration 2.2.7.3: Satellite image of the fires from NASA.....	34
Illustration 2.2.7.4: Areas (with a point in its center) measured by the SEVIRI radiometer.....	34
Illustration 2.2.7.5: Rotation error and skew.....	35
Illustration 2.2.7.6: Rotation error and skew.....	35
Illustration 2.2.7.7: Raster for brightness temperature (3.9um), instant before the fire.	35
Illustration 2.2.7.8: Raster for brightness temperature (3.9um), instant after the ignition.....	35
Illustration 2.2.7.9: Beginning of the fire (11:00 22/07/2012).....	36
Illustration 2.2.7.10: Instant just before the beginning of the fire (10:45 22/07/2012).....	36
Illustration 2.2.7.11: IR 3.9 um brightness temperature with elevation (10:45 22/07/2012).....	37
Illustration 2.2.7.12: Brightness temperature (ir 3.9 um) at dawn (08:30 22/07/2012) with elevation (meters).....	37
Illustration 2.2.7.13: Brightness temperature (ir 3.9 um) at dawn (11:00 22/07/2012) with elevation (meters).....	38
Illustration 2.2.7.14: Brightness temperature difference (IR 3.9um) before and after the beginning of fire.....	39
Illustration 2.2.7.15: Brightness temperature difference (IR 3.9um) between 05:00 and 15:00.....	39
Illustration 2.2.7.16: Difference in brightness temperature between before and after the ignition (10:45 22/07/2012 - 11:00 22/07/2012).....	40
Illustration 2.2.7.17: Difference in brightness temperature between before and after the ignition (10:45 22/07/2012 - 11:00 22/07/2012).....	41
Illustration 2.2.7.18: Difference in brightness temperature between before and after the ignition (10:45 22/07/2012 - 14:00 22/07/2012).....	42
Illustration 2.2.7.19: Brightness temperature before the ignition of the fire (10:45 22/07/2012).....	43
Illustration 2.2.7.20: Brightness temperature after the ignition of the fire (11:00 22/07/2012).....	43
Illustration 2.2.7.21: Atmospheric absorption bands (Carbon Dioxide highlighted).....	44
Illustration 2.2.7.22: Satellite high resolution image of 2012 North Catalonia forest fire.	44
Illustration 2.2.7.23: Visual light inside the channel 006.....	44
Illustration 2.2.7.24: SEVIRI visual response for HRV, VIS006 and VIS008.	46
Illustration 2.2.7.25: Reflectivity index before the beginning of the fire (vis006).....	46
Illustration 2.2.7.26: Reflectivity index after the beginning of the fire (vis006).....	46
Illustration 2.2.7.27: Spectral response difference in 15min (10:45 22/07/2012 - 11:00 22/07/2012).	47

Illustration 2.2.7.28: Spectral response difference in 4 hours (10:45 22/07/2012 - 14:45 22/07/2012).....	47
Illustration 2.2.7.29: Brightness temperature (3.9um) after 9 hours (19:15 22/07/2012)	48
Illustration 2.2.8.1: Brightness temperature standard deviation at the beginning of the LaJonquera forest fire.....	50
Illustration 2.2.8.2: Fire detect by thresholding contextual algorithm (11:00 22/07/2012).....	50
Illustration 2.2.8.3: Fire detected by thresholding contextual algorithm (20:00 22/07/2012).....	50
Illustration 2.2.8.4: Fire detect by thresholding contextual algorithm over the terrain (11:00 22/07/2012).....	51
Illustration 2.2.8.5: 2 NxN matrix in a sudden change of temperature.....	52
Illustration 2.2.9.1: Brightness temperature of 4 different points during 10 days.....	53
Illustration 2.2.9.2: Channel 4 (IR3.9) during in 4 points during the fire.....	54
Illustration 2.2.9.3: Brightness temperatures in a fire spot in Colomers (Girona, Spain).....	55
Illustration 2.2.9.4: Brightness temperatures in a fire spot in Ronhac (Marseilles,France).	55
Illustration 2.2.9.5: Reflectance by visual channels during forest fire in Colomers (Girona).....	56
Illustration 2.3.1.1: Take-off from ground.....	58
Illustration 2.3.1.2: Gaining altitude (ground too close to analyze).....	58
Illustration 2.3.1.3: Optimal elevation reached. Analysis begins.....	59
Illustration 2.3.1.4: Recording the ground. Using balloon as lifejacket while analyzing the terrain.	59
Illustration 2.3.1.5: UAV is unplugged from balloon and begins descend.....	60
Illustration 2.3.1.6: The UAV descends with a parachute.....	60
Illustration 2.3.1.7: UAV sweeps the area of interest repeatedly.....	60
Illustration 2.3.1.8: The UAV returns to the origin point.....	60
Illustration 2.3.2.1: The Atmos-7 UAV system.	61
Illustration 2.3.3.1: Shift error.....	62
Illustration 2.3.3.2: Scale error.....	62
Illustration 2.3.3.3: Vertical/Horizontal error.....	63
Illustration 2.3.3.4: Skew.....	63
Illustration 2.3.3.5: Projection distortion.....	63
Illustration 2.3.3.6: Skew.....	63
Illustration 2.3.3.7: Earth curvature distortion.....	64
Illustration 2.3.3.8: Terrain relief distortion / displacement.....	64
Illustration 2.3.3.9: Example of terrain relief displacement.....	64
Illustration 2.3.4.1: Radiometer field of vision.....	65
Illustration 2.3.4.2: Image generated by the thermal imaging camera Miricle.....	66
Illustration 2.3.4.3: Spacial resolution and Field Of View at 20km for the Miricle 100k.....	67
Illustration 2.3.4.4: NEC F30 thermal infrared imaging camera.....	68
Illustration 2.3.4.5: Thermal image from NEC F30.....	68
Illustration 2.3.4.6: Visible image (visual image) from NEC F30.....	68
Illustration 2.3.4.7: Spacial resolution and Field Of View for F30.....	70
Illustration 2.4.1.1: Infrared image. Fire describing a perimeter.....	72
Illustration 2.4.1.2: Forest fire seen by different wavelengths.....	74
Illustration 2.4.1.3: Surface and crown fire.....	74
Illustration 2.4.1.4: Surface fire.....	74
Illustration 2.4.1.5: Perimeter stretched by the wind and the slope (inclination).....	76
Illustration 2.4.1.6: Different perimeters of different vegetation under different wind speed.....	76
Illustration 2.4.1.7: Fire crossing the Highway N-II AP-7 (Sample Data Zone).....	76
Illustration 2.4.1.8: Embers from a forest fire.....	76
Illustration 2.4.1.9: Firebrand particles under strong wind creating multiple spots.....	77

Illustration 2.4.1.10: Firebrand particles under soft wind creating a spot.....	77
Illustration 2.4.2.1: GIMP application and its palette.....	77
Illustration 2.4.2.2: Hue described by degrees.....	78
Illustration 2.4.2.3: Relation between hue, value and saturation.....	78
Illustration 2.4.2.4: The hue of the fire dominates.	79
Illustration 2.4.2.5: Plumes created by wildfires from high altitude.	80
Illustration 2.4.2.6: Smoke from the fire at high altitude.....	81
Illustration 2.4.2.7: Pattern that identifies smoke.....	82
Illustration 2.6.1.1: Geographical location of fire lookout towers.....	85
Illustration 2.6.1.2: Fire lookout towers in natural park (Parc del Montnegre i el Corredor)......	85
Illustration 3.1: Diagram behind the analysis related to visual imagery.....	88
Illustration 3.2: Diagram behind the analysis related to thermal infrared imagery.....	89
Illustration 3.3: Diagram behind the matching code.....	89

Index of Equations

Text 2.2.3.1: Formula to calculate radiation from pixel count.....	25
Text 2.2.3.2: Formula to calculate Brightness Temperature from Radiance.....	26
Text 2.2.3.3: Radiance to reflectance equation.....	27
Text 2.2.5.1: Conditions to detect a wildfire.....	28
Text 2.2.6.1: function to determinate the possibility of wildfire.....	30
Text 2.2.8.1: Last equations for thresholding contextual algorithms.....	48
Text 2.2.8.2: Other equations for thresholding contextual algorithms.....	49

Index of Tables

Table 2.2.2.1: List of geosynchronous radiometers.....	19
Table 2.2.3.1: Channels in SEVIRI.....	22
Table 2.2.7.1: Largest forest fires in Catalonia.....	33
Table 2.2.7.2: Visual channels in SEVIRI.....	45

1. Introduction

It is important to highlight that less than 10% of forest fires are caused by the nature [ref.1] herself. Most of them are man-made disasters. The vast majority of wildfires are caused by forest work, agricultural work or criminal arson. It is the duty of mankind to prevent, monitor and minimize the forest fires and its adverse effects. All wildfires are projected to increase year after year. Forest fires not only increase because of the established trend of hotter summers and higher temperatures year after year, but also because of the gradual abandonment and depopulation of the forest by the rural jobs. The farmers, shepherders, woodcutter,... used to remove all the accumulated fuel inside and around the forests. With the countryside empty of those who could create firewalls to the flames, the fire is harder to spot, stop and extinguish [ref.1].

And summer after summer the same disaster appears. The well being of the forest and, therefore the prevention of fires, is linked to the well being of the populations on it. And not far a way, the writer of this project who live in the north east side¹ of Catalonia witness himself these events powerless. Even today and every summer forest fires are an expected disaster which is hard to fight despite being a repetitive problem. Despite public awareness, the closing of forests to the people, harsher punishments, the deployment of the military, every summer several wildfires takes place in many countries regardless their means to detect, fight, trace the fire. Irreplaceable ecosystem are lost and the damage is a burden for the local community as well as for the public institutions that must pay

¹ The North East side of Catalonia is know by its propensity to forest fires and strong winds.

for the reparations, although the loss of human lives can never be repaid. And beyond the local and visible effects on the ground where the forest fire or wildfire has taken place, it is important to locate, measure, calculate, compare its magnitude in order to disclose a more invisible and subtitle effect on climate change, air quality, fragile ecosystems, etc... Forest fire might produce an indirect domino² effect which produce at its own time a new emergency related to the fire among other factors. Wildfires, however, are also a part of natural cycles; they regulate the existing fuel in forest and they stabilize biologic diversity. Therefore, it is crucial to measure data from the fire with knowledge and balance.

Of course there are many ways to approach this project and its mission: Satellites, UAV, manned planes –conventional planes with sensing payloads- and fire lookout towers against forest fires. This work observes the diverse ways to accomplish the mentioned task and compares among themselves. However, this project will focus on the combination of information from the devices such as cameras or radiometers installed as payloads in UAV.

To summarize the intent of this project, there is a need to have a -near- real time or even precise system that is able to do all the fire forest related tasks assigned. However, as one might know, the remote sensing provided by satellites is a double edge sword. The satellite-based instruments have lower spatial and temporal resolution but they are able to sense continuously a large area -almost 1/3 of earth's surface if the satellite is geosynchronous-. But even LEO (Low Earth Orbit) satellite-based instruments have lower resolution than a drone-based ones.

There is a detail in the UAV option, that all the other systems fail to avoid. The UAV is the option that avoids more infrastructure³ and it might be less intrusive and sustainable than all other methods. A drone carrying a payload might be the most precise and the most selective of all methods named while being free of all the infrastructure like a ground station, money and fuels related to the other monitoring methods, however, might be arguable that very small lookout tower could use less in fracture.

1.1. Mission

The main target of this work is to analysis how the wildfires -forest fires- can be detected, prevented or monitored or even predicted using a UAV with visual camera and infrared camera attached. The

² The domino effect is described in the infocat INFOCAT (Pla d'emergencies per INCendis FOrestals a CATalunya, emergency plan against forest fires in Catalonia).

³ Aircraft-borne sensors require airport, heliport, tracks,... space-borne sensors require satellite and ground stations.

others means to deal with fire are like fire lookout towers, planes and satellite are compared to some extend to prove its usefulness.

The basic principle of this project and the previous to this one is to design a code or an algorithm that is able to monitor and measure fire forest from a UAV and it must be able to count the area that has been burn by the forest fire. There are many ways to accomplish that but this project focus how to extrapolate code and data from the space-borne radiometers to commercial visual and infrared cameras installed in UAV or drones as sensing payloads. One third option is to use a combination of UAV and satellite data.

While this extrapolation is done, a comparison will emerge between the different way to monitor or track a fire given a better understanding of all the point of view to analyse the fire.

1.2. Scope

The scope of this project is to study the different ways to detect a fire to compare their cost and parameters like temporal and spacial resolution. The second idea is to begin to search for code or algorithms that will be able to measure burned areas and quantify them with precision given imagery provided by the payload from drones -small vehicle without pilot or crew-. This project doesn't give apply the theory but study its deployment and inner workings. The company that provides the UAV is Catalan and the most of satellite-based data is from Catalonia, however, there are few forest-fires -or not enough- and the writer of this project might borrow some information about fires outside Catalonia -from France-. The present project will focus mainly in this geographical zone. This implies that the satellites used have to sense and record a certain part of the globe. In that case, Western or Central Europe.

1.3. Hypothesis

Many articles has been written about the use of satellite to detect and monitor fires in land. There are also many articles and thesis about it. The main hypothesis is that despite all the satellites geostationary and non-geostationary and its data a more accurate way to monitor forest fires in real

time are UAV⁴ in different elevation above the fire (10-25 km altitude). These are the hypothesis:

1. It is possible to extrapolate data from satellite.

The imagery or data that comes from drones at high altitude while recording a forest fire is extremely scarce. Part of this work gets information from satellites in order to extrapolate patterns to drone information. The hypothesis is that there is data from satellite can be used in order to not only detect fires but to measure burned areas.

2. Faster monitoring.

There is a time between an event or a change in the forest fire and the instant when the final user is able to grasp such information. The second hypothesis is that the information received from drones is faster than the ones coming from manned air planes, lookout tower and satellite.

3. Better prediction.

The third hypothesis is that a drone at a certain altitude carrying certain sensing instruments is able to deliver information that might provide better prediction than planes, satellites, even lookout towers.

4. Better measurements

This hypothesis states that even from an altitude that ranges from 10km to 20km and a conventional range of sensor, the measurements are better meaning that it has better temporal and spatial resolutions as well as sensitivity.

5. Less false positive alerts.

In many documents and charts, there is the assumption that a small percentages of false positive alarms occurs in after applying algorithms to received data from satellite-borne sensors.

6. Cheaper than permanent Fire Lookout Towers, Manned air-planes and satellite-based remote sensing

While each way of obtaining data has its strength and weakness and none dismisses another, it is important to know if the benefits of UAV-based remote sensing instruments are worth the efforts. To sum up this hypothesis, there should be a study of viability that supports this option.

4 The UAV are Unmanned Air Vehicle, however, that included also one of the stage when the UAV is lifted by a aerostatic balloon.

2. Study of the different analysis

2.1. Tools for forest fire prevention detection and monitoring.

There are several tools to prevent, detect and monitor not only active forest fires but also burned areas. Depending on their weight and if they are active⁵ or not, some positions or vehicles certain payloads or not:

- Satellite-borne:
 - Radiometers.
 - Radars (SAR).
 - Cameras.
- Unmanned Air Vehicle (UAV):
 - Visual Camera (visual band).
 - Infrared Camera.
- Manned aircraft borne:
 - Camera.
 - Radiometers.
 - Radar⁶(SAR).
- Fire lookout tower:
 - Human fire lookout.
 - Visual camera.
 - Infrared camera.

5 When a remote sensing instrument is described as active, this makes reference to active radars that do emit radio wave in order to detect their echo.

6 One of the most usually carry payload by aircraft are radars. Radar are no able to measure fire or temperature, but radars are able to scan the terrain and analyse the backscattering of the emitted signal.

2.2. Space-borne analysis

There are many measuring instruments that can be carried by the satellites. This is determined by their weight, cost, maintenance. The question is which and how are they able to detect and measure an active fire taking place on the Earth's surface.

2.2.1. Radar analysis

The radar implies an active sensing instrument. The radar backscatter is the relation between the signal and its reflection. Radar backscatter (σ) measurements over forested areas depend on vegetation type, species, and structure, vegetation biomass, topography and surface roughness and canopy height; flooding and the presence or absence of standing water, and moisture. The radar backscattering is used also to detect different types of vegetation. The three sources of moisture variation may contribute to the forest radar backscatter: the forest floor, the canopy and the environmental conditions. In other words, when a forest is burned, the moisture and the quantity of water inside the plants changes, therefore, the radar backscatter index change, allowing the radar to identify burned area from not burned areas. The illustration 2.2.1.1 shows the three stages of the forest fire.

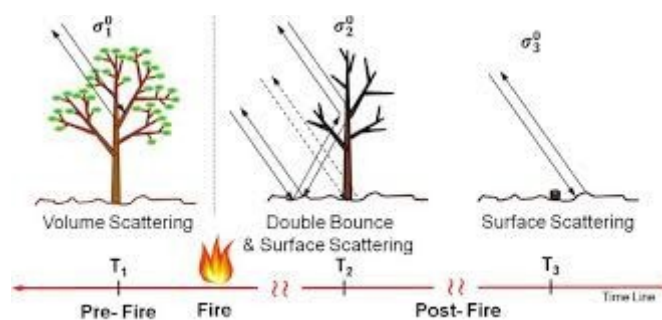


Illustration 2.2.1.1: Backscatter depending on the fire.

However, there are no SAR type of radars in MSG (Meteosat Second Generation), JAMI or GOES; satellite-borne SARs are placed in lower orbits to sweep the surface as they orbit around the Earth making a real time tool for a specific area.

2.2.2. Space-borne radiometric analysis

Radiometry

It is stated that all bodies that have a temperature above absolute zero (0°K) emit a certain electromagnetic wave and it will be emitted outside if the temperature is lower; that's what is called the black body theory. The black body is the theoretical -no real- body that absorbs all the electromagnetic spectrum, all colors included, that's why it is called black body. In real life, there are just grey bodies. Of course the human eye cannot perceive this -almost infrared- black body radiation at very low temperature if the temperature is not high enough. If the temperature was high enough the body will glow red and if even hotter white. Of course radiation have an spectrum and amplitude depending on the temperature of the body [ref.3].

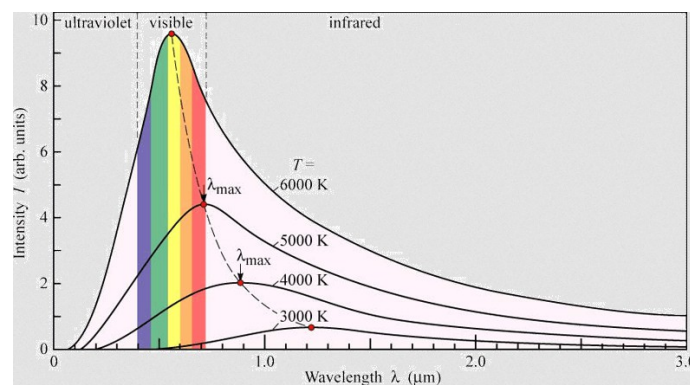


Illustration 2.2.2.1: Black body radiation and the visible spectrum.

The illustration 2.2.2.1 shows how to relate the black body radiation and the visual wavelength. As the temperature grows, the peak wavelength changes and that change the color of the heated body.

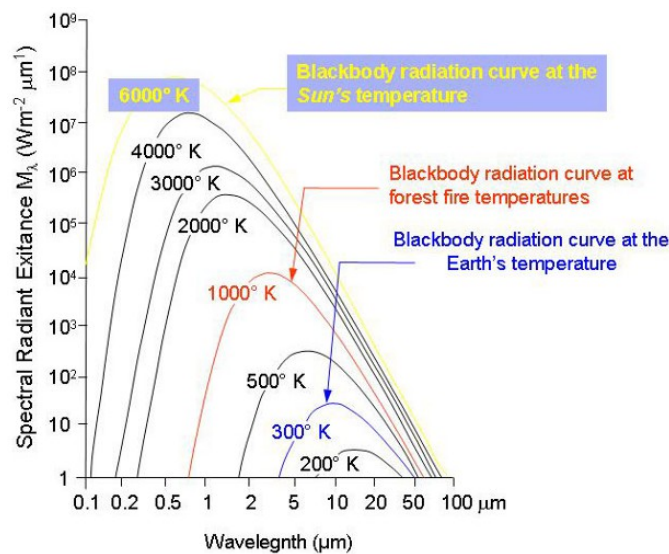


Illustration 2.2.2.2 Relation between black body radiation and brightness temperature.

A fraction of the heat produced by the forest fire escapes as radiation. The body that is burning increase its temperature and emits that black body radiation towards other cooler bodies. Another part of the energy transforms into heat convection and heat conduction. Knowing the relation between the temperature of the “black body” and its radiance, it is possible to calculate the brightness temperature.

Radiometers are used to detect brightness temperature, or in other words, radiometers measure the radiance, noise equivalent power, from a body that can be indicator of the temperature of a body of mass and related to a certain area. The illustration 2.2.2.2 displays the relation between radiance exitance (power per surface of a certain wavelength) with the spectrum, or how certain temperature are related to the spectrum. It is just the amplification of the illustration 2.2.2.1. This illustration highlights the importance of certain wavelengths to detect forest fires and its temperatures. With the interest of analysing and detecting forest fires in mind, there should be radiometers that measure such wavelengths with as much accuracy and frequency as possible. So there should be a radiometers that constantly monitors a zone that might suffer a forest fire or how a fire is developing.

Radiometers

The radiometers are tools that are used to measure brightness temperature with certain wavelengths. These are heavy devices and they are carried by usually satellites -or manned aircrafts-, in other

words, the possibility of radiometers being transported by a drone is discarded. There are two kind of satellites depending on the orbit, or in other words altitude and scanning frequency: geosynchronous and the other ones (polar, MEO,LEO).

Satellites with geosynchronous orbits always face the same surface of the earth continuously, their spacial resolution is lower compared to the satellites with lower orbits but its temporal resolution is better and they provide a near real time data. On the other hand, the other satellites with lower orbits may have better spacial resolution but worst temporal resolution as they keep orbiting the earth. These satellites -not geosynchronous- and their instruments like MODIS, AVHRR, ASTER and Landsat that are certainly used for fire detection and fire monitoring but they have a very low time resolution because they are not geosynchronous -they describe polar orbits-.

MODIS or AVHRR might be used to confirm and correct the place of the temperatures analysed and the burned area while providing a better sensibility after a certain time -days or more-.

It should be added that even when the satellite face one area constantly, the radiometer requires some time to sweep an target area. The explanation for the time is based on the inner workings of the radiometers to sweep the partial surface of earth they face. This is a critical factor because all the delay causes by this “full disk coverage”, its data transmission to the ground segment and the remaining time to create a chart for the final user describes a delay which determine its utility for a near real time monitoring of wild fires. The table 2.2.2.1 describes several geosynchronous satellites with radiometers able to detect fires. The GOES-11 and GOES-12 are discarded because of the period between the provided images. On the other hand, SEVIRI (Spinning Enhanced Visible and InfraRed Imager) and JAMI (Japanese Advanced Meteorological Imager) have period of time shorter that allow them to be considered used for a near real time system or algorithms.

Satellite Sensor	Position	Active Spectral Bands	Fire IFOV (km)	SR (km)	Full Disk Coverage ⁷	3.9 um Saturation Temperature (K)	Minimum Fire Size at Equator ⁸ (at 750°K)(ha)
MSG ⁹ 8 (SEVIRI)	3.5°E	1 HRV 2 visible 1.6, 3.9, 10.8	1.6 4.8 4.8	1.0 3.0 3.0	15 min	≈335°K	0.22
MSG 9 (SEVIRI)	9.5°E	1 HRV 2 visible 1.6, 3.9, 10.8	1.6 4.8 4.8	1.0 3.0 3.0	15 min	≈335°K	0.22
MSG 10 (SEVIRI)	0°E	1 HRV 2 visible 1.6, 3.9, 10.8	1.6 4.8 4.8	1.0 3.0 3.0	15 min	≈335°K	0.22
GOES-11 (Imager)	135°W	1 visible 3.9 um 10.7 um	1.0 4.0(8.0)	0.57 2.3	3 hours	≈322°K	0.15
GOES-12 (Imager)	75°E	1 visible 3.9 um 10.7 um	1.0 4.0(8.0)	0.57 2.3	3 hours	≈335°K	0.15
MTSAT-1R (JAMI)	140°E	1 visible 3.9 um 10.7 um	0.5 2.0		< 24 min	≈320°K	0.03

Table 2.2.2.1: List of geosynchronous radiometers.

Of course, the instruments not only must have a small delay but also they must focus towards the interested area. MSG-8, MSG-9, MSG-10 are valid but the best one in terms of spacial resolution is the MSG-10.

⁷ The full disk coverage is the periodic time the radiometer needs to sweep the entire surface under its field of view.

⁸ This is a theoretical min size of the forest fire that the radiometer is able to detect.

⁹ MSG is the acronym for Meteosat Second Generation.

2.2.3. SEVIRI

The Spinning Enhanced Visible and Infrared Imager -also known as SEVIRI- is the MSG (Meteosat Second Generation) satellite's main payload and it is the optical imaging radiometer. It has 12 spectral channels and it has the unique capabilities for cloud imaging and tracking, fog detection, measurement of the Earth-surface and cloud-top temperatures. The interesting feature for fire detection is the measurement of Earth-surface temperatures.

This is the “fastest” radiometer with commercial data that can be acquired. From ESA web page:

Spectral range:

- 0.4 – 1.6 μ m (4 visible/NIR channels). Used to detect reflectivity of sun radiation upon the movement of clouds or plumes of fire. Only valid under sun light.
- 3.9 – 13.4 μ m (8 IR channels) (Used to detect temperature anomalies from noise equivalent power).

Resolution from 35 800 km altitude¹⁰ (See illustrations 2.2.3.4 and 2.2.3.5):

- 1 km for the high-resolution visible channel.
- 3 km for the infra-red and the 3 other visible channels.

Focal plane cooled to 85/95 °K.

One image every 15 min (245 000 images over 7 yr nominal lifetime).

Instrument mass: 260 kg.

Dimensions:

- 2.43 m high.
- 1 m diameter without Sun Shield.

Power consumption: 150 W.

Data rate: 3.26 Mbit/s.

¹⁰ This is the best spatial resolution at the equator, not the average resolution.

Channel number	Spectral band (μm)	Characteristics of Spectral Band (μm)	Main observational application
----------------	---------------------------------	--	--------------------------------

		λ_{cen}	λ_{min}	λ_{max}	
1	VIS0.6	0.635 μm	0.56 μm	0.71 μm	Surface ¹¹ , clouds, wind fields
2	VIS0.8	0.81 μm	0.74 μm	0.88 μm	Surface, clouds, wind fields
3	NIR1.6	1.64 μm	1.50 μm	1.78 μm	Surface, cloud phase
4	IR3.9	3.9 μm	3.48 μm	4.36 μm	Surface, clouds, wind fields
5	WV6.2	6.25 μm	5.35 μm	7.15 μm	Water vapor, high level clouds, upper air analysis
6	WV7.3	7.35 μm	6.85 μm	7.85 μm	Water vapor, atmospheric instability, upper-level dynamics
7	IR8.7	8.70 μm	8.30 μm	9.1 μm	Surface, clouds, atmospheric instability
8	IR9.7	9.66 μm	9.38 μm	9.94 μm	Ozone
9	IR10.8	10.80 μm	9.80 μm	11.80 μm	Surface, clouds, wind fields, atmospheric instability
10	IR12.0	12.00 μm	11.00 μm	13.00 μm	Surface, clouds, atmospheric instability
11	IR13.4	13.40 μm	12.40 μm	14.40 μm	Cirrus cloud height, atmospheric instability
12	HRV	Broadband (about 0.4 – 1.1 μm)			Surface, clouds

Table 2.2.3.1: Channels in SEVIRI.

The table 2.2.3.1 shows the difference channels provided by the SEVIRI radiometer. There are, however, one or two channels that are specially interesting for the detection of forest fires. The channel 4 (IR3.9 μm) -as well as the channel 9 (IR10.8 μm)- is not absorbed by the atmosphere and have a linear sensibility in order to calculate the temperature.

¹¹ Surface Temperature. Channels that are able to measure

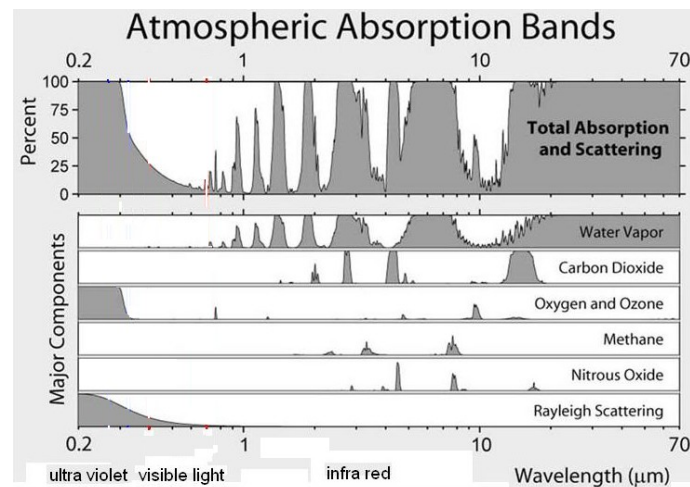


Illustration 2.2.3.1: Atmospheric absorption for different wavelength.

The illustration 2.2.3.1 shows which wavelengths are being attenuated by the atmosphere. Any fire product (system able to detect or track fire) focus on the information that comes from the surface.

Of all channels the IR3.9 -or channel 4 (Infrared 3.8 μ m)- is the more sensible one to temperature changes. The IR10.8 -or channel 9 (Infrared 10.8 μ m)- serves as an auxiliary band; the IR3.9 channels is not as linear as the IR10.8 channel and to give a valid lecture the difference $T_{IR3.9} - IR_{10.8}$.

Different wavelength have different reflections and attenuation in the atmosphere. Each one highlights a specific magnitude. The key question is how it is possible to detect a fire with more accuracy given that information and which wavelength should be observed.

The brightness temperature is not the temperature of the fire. The brightness temperature depends on the size of the fire and the temperature or intensity of a fire. A large fire -a large area of fire- would have a higher brightness temperature than small fire. However, if the small fire has a high intensity¹² it would have the same brightness temperature as the large fires and in this case both small and large fires would affect the same number of pixels with equal intensity. The radiometer like SEVIRI -or any other radiometer like MODIS or AVHRR- deliver the brightness temperature of an area which can be as large as 25km² (5km x 5km).

¹² The intensity of the fire depends on the fuel that is being burned and how it is burned.

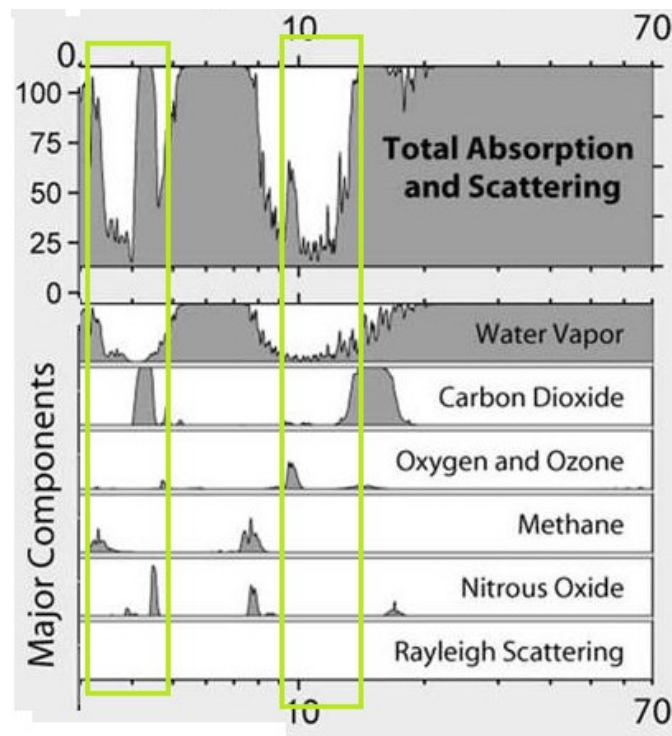


Illustration 2.2.3.2: Wavelengths not affected by atmospheric absorption nor scattering.

The illustration 2.2.3.2 show how the atmosphere absorption and scattering describe two windows where the radiometry is able to obtain information from the Earth's surface.

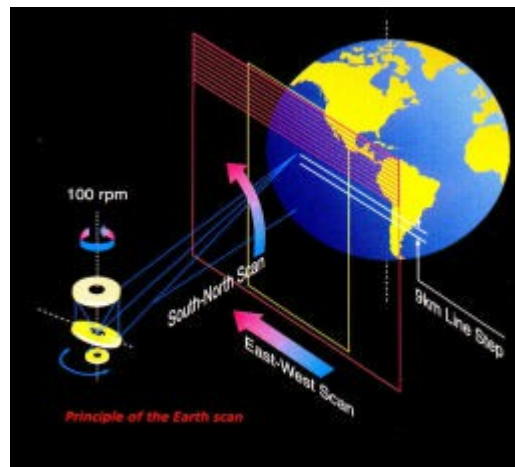


Illustration 2.2.3.3: Scheme of the SEVIRI radiometer.

The illustration 2.2.3.3 shows how the radiometer sweeps with West-East lines from South to North.

Later, the data displayed will reveal that the data isn't West-East lines perpendicular to the North-West axis. The curvature of the earth and its rotation might expand and incline some regions so that this will also affect the spacial resolutions in certain areas and the rotation. In the illustration 2.2.3.5 and 2.2.3.4, the spatial resolutions vary because of the curvature of the Earth. The darkest gray zone has a spatial resolution of 3.1 km, that's the best resolution for infrared wavelength channels. The spatial resolution for the next lighter gray zone are 4km, 5km, 6km, 8km and 11km. For example, in the Iberian peninsula, inside the green rectangle, the north-south resolution is 5km while the West-East resolution is 4 km.

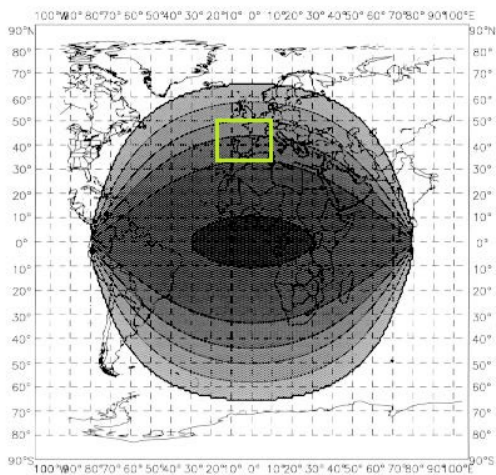


Illustration 2.2.3.5: North-South level 1.5 ground resolution.

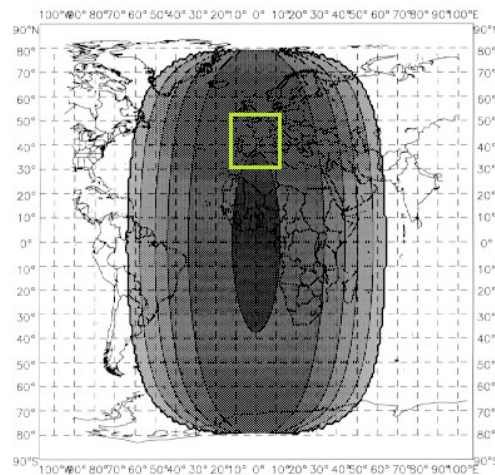


Illustration 2.2.3.4: West-East level 1.5 ground resolution.

The SEVIRI doesn't provide the brightness temperature nor the radiance. SEVIRI provides pixel counts and self calibrates. SEVIRI uses the deep space as a cold source and an internal black body as a warm source for the calibration [ref.5].

$$L [mW^{-2} sr^{-1} (cm^{-1})^{-1}] = cal_{offset} + (cal_{slope} \cdot Level\ 1.5\ Pixel\ Count)$$

Text 2.2.3.1: Formula to calculate radiation from pixel count.

The formula 2.2.3.1 transforms the pixel counts to radiation. The calibration keeps changing very slowly for each channel, almost constant. Then, once the radiation is obtained, it is possible to get

the brightness temperature. All the calibration information is inside the netCDF file that describes how it changes along the time [ref.6]. The calibration doesn't change frequently. Calibration slope and calibration offset keep the value for months¹³. In order to obtain the brightness temperature the formula

$$T_{brightness} = \frac{\left(\frac{c_2 v_c}{\log \left(1 + \frac{c_1 v_c^3}{R} \right)} \right) - B}{A}$$

Text 2.2.3.2: Formula to calculate Brightness Temperature from Radiance.

Where the c_1 and c_2 are

$$c_1 = 2 h c^2 \quad c_2 = \frac{h c}{k}$$

h is the Planck constant ($6.62607004 \times 10^{-34} \text{ m}^2 \text{ kg} / \text{s}$), the c is light speed (299792458 m/s) and k is the Boltzmann constant ($1.38064852 \times 10^{-23} \text{ m}^2 \text{ kg s}^{-2} \text{ K}^{-1}$). And v_c is the central wavelength of the channel and A and B are correction coefficients.

However, SEVIRI not only provides the brightness temperature from the Earth surface but also the reflectance from visual channels. The three visual channels 01, 02 and 03 that do not observe the brightness temperature but how much light with a certain bandwidth is reflected. To understand this channels is necessary to take in account the sun path which includes solar zenith angle, date and time to understand how much light is reflected regardless the sun position. Unfortunately, this has a mayor flaw in the detection of the fire. This channels are only useful during daylight. The idea behind the use of this channels is the detection of changes caused by the plumes of smoke. The formula required to obtain the reflectance is much complex because it requires the sun path. The equation 2.2.3.1 calculated the radiance from pixel count (SEVIRI internal units). Then the equation 2.2.3.3 calculates the reflectance from the radiance.

¹³ The slope is 3.6585 and the offset is -0.1866. These values are repeated with all the forest fire data.

$$r_{\lambda} = \frac{\pi \cdot R_{\lambda} \cdot (d_{\text{earth-sun}}(t))^2}{I_{\lambda} \cdot \cos(\theta_{\text{zenith}}(t, \text{lon}, \text{lat}))}$$

Text 2.2.3.3: Radiance to reflectance equation.

where

R_{λ} is the radiance that reaches the SEVIRI radiometer.

$d_{\text{earth-sun}}(t)$ is the distance between sun and earth in astronomical units.

I_{λ} is the band solar irradiance at one astronomical units.

$\theta_{\text{zenith}}(t, \text{lon}, \text{lat})$ is the zenith angle at an specific time and place with a longitude and latitude.

2.2.4. Fire detection algorithms

Given the brightness temperature -from radiance- associated to certain wavelengths, there are two approaches on how to detect an anomaly that might indicate a fire on the Earth's surface temperature or ground temperature¹⁴, so there are two main types of algorithms to detect a wildfire.

- Thresholding contextual algorithms
- Thresholding multi-temporal algorithms.

¹⁴ Ground temperature: this is the term opposed to the temperature detected in the upper side of the clouds or in the air. The ground temperature refers to the temperature of the ground or the nearest to the surface.

2.2.5. Thresholding contextual algorithms

The contextual algorithm compares the temperature from one pixel and the temperature that surrounds this spot. It compares the temperature from one spot with the average temperature of the matrix. If one pixel contains a temperature higher than the ones' that surround it then it is considered a hot spot and a possible wildfire. Of course, this algorithm takes into account the deviation of the matrix. The $T_{3.9\mu m}$ quickly escalates when the temperature rises unlike the $T_{10.8\mu m}$ that has a more moderate sensibility, that's why the difference between the temperatures. This difference give also the information about the real temperature of one spot. The matrix have usually the dimensions of 3x3 pixels [ref.2].

$$T_{3.9\mu m} > \mu_{3.9\mu m} + f \cdot \sigma_{3.9\mu m}$$

$$T_{3.9\mu m} - T_{10.8\mu m} > \mu_{dif} + f \cdot \sigma_{dif}$$

Text 2.2.5.1: Conditions to detect a wildfire.

where

T is the temperature for pixel

μ is the average or mean for the NxN temperature matrix.

σ is the standard deviation for the NxN temperature matrix.

f is a factor that determines the sensibility of the thresholds.

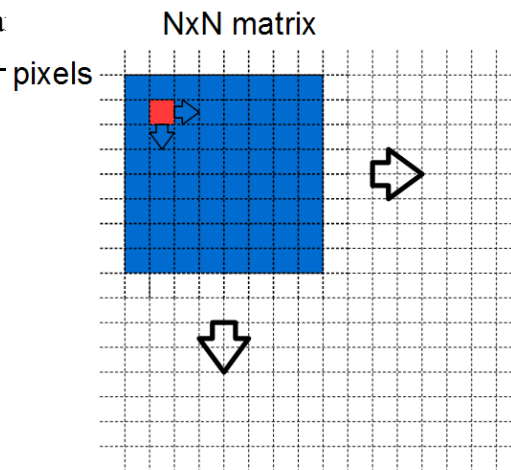


Illustration 2.2.5.1: Thresholding contextual algorithms sweeping process.

The first condition of the equations in the text 2.2.5.1 confirms that larger amount of radiance from this channel implies a source of higher temperature. The second condition takes into account the fact that the two different channels -channel 04 (IR3.9) and channel 09 (IR10.8)- have different sensibility of temperature and this implies that the difference between the two is proportional to the brightness temperature of the “gray body”.

The illustration 2.2.5.1 shows the sweeping process that the thresholding contextual algorithm executes. The matrix with a NxN number of pixels sweeps across any given number of pixels and in every step, all the pixels are analysed. If one pixel or more are above the average plus a certain deviation, it would be considered that a forest fire is taking place. The problem with this kind of algorithms is that sometimes, in some pixels like deserts or human spots, there are points usually hot surrounded by colder pixels around them without any wildfire. This hot pixel surrounded by cold pixels might provoke a false positive alarm of a forest fire. Depending on the pixel size and the NxN (pixels x pixels) size of the matrix, elevation of the terrain and controlled human heat source -like a chimney-, it might create false positive alarms. In flat opposition, if the matrix is too small and the temperature from all the pixels are high and the fire is not intense, it would miss the fire alarm.

2.2.6. Thresholding multi-temporal algorithms

The multi-temporal algorithm, instead of calculating the average and the standard deviation from a matrix and of to observe the same spot during a long time and compare the current pixel temperature with the history of that spot.

$$X_{MIR}(x, y, t) = \frac{T_{MIR}(x, y, t) - \mu_{MIR}(x, y)}{\sigma_{MIR}(x, y)}$$

Text 2.2.6.1: function to determinate the possibility of wildfire.

where

T is the temperature for pixel at the t time in the (x,y) position.

μ is the average or mean for the pixel at the (x,y) position.

σ is the standard deviation for the pixel at the (x,y) position.

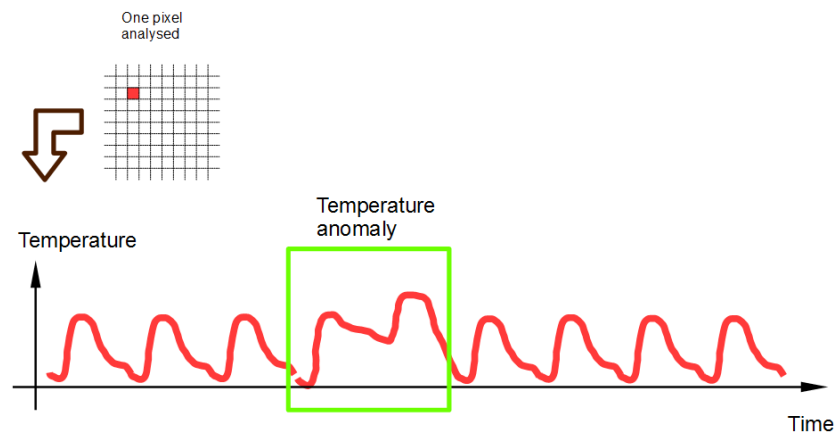


Illustration 2.2.6.1: Temperature from a pixel that suffers the fire anomaly.

The illustration 2.2.6.1 shows a very ideal oscillation of the temperature with a increase of temperature caused by a fire inside the green square. The temperature of a pixel usually follows an oscillation. This oscillation have different forms depending on the analysed spot but it is repeated every day because of the sun path. The illustration 2.2.6.1 shows a daily oscillation but it should be added that not visible clouds can disrupt this oscillation.

The multi-temporal is better than the contextual algorithms because it considers the history of the spot where the temperature has been measured. It also increases the complexity of the analysis because of the need to store all the historical data of every single spot. The algorithm also must observe the changes of temperature because of cloud and sun path¹⁵ during the year. However, this method doesn't contemplate the events sources of heat that are not periodical like industrial chimneys or heat from urban or industrial centres. The main problem is how to define threshold enough low to avoid missing a fire but high enough to avoid false positive alarms.

2.2.7. Study Case and Data samples : Forest fires in North Catalonia.

Fortunately, there is radiometric and visual information related to a relatively recent fire in North Catalonia. This data belongs to the SEVIRI and it contains, the 3.9 μm , 10.8 μm , 13.4 μm infrared

¹⁵ The Sun path refers to the apparent significant seasonal-and-hourly positional changes of the sun (and length of daylight) as the Earth rotates, and orbits around the sun.

wavelengths and the $0.6\mu\text{m}$ visual brightness temperature. The spacial resolution found in the samples provided belongs to the geographical range where the Iberian peninsula is located; this spacial resolution is 5km or more.

The unfortunate incident took place on July the 22nd: Two wild fires begin at the border between France and Spain, one started in La Jonquera and later on another in Portbou. The first started during midday; it affected 13,800 hectares -included in this are some 3,000 hectares of crops that did not burn-, 19 municipalities and caused two deaths. The fire of Portbou began at 19:00 and was controlled in a few hours, burning 50 hectares and killing two people trying to flee the encroaching flames by jumping from the cliffs into the sea. In total, 3,200 residents were left without electricity and 1,700 without phone.

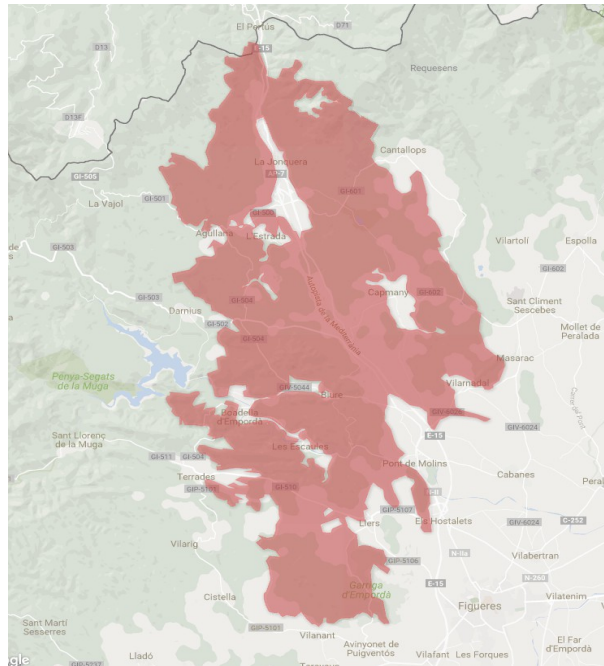


Illustration 2.2.7.1: Precise burned area by the fire.

This LaJonquera fire was one of the largest fire in almost 2 decades. Since 1994, there hasn't been a larger forest fire that has burn more hectares. In Catalonia the 40 largest forest fires have consumed the 75% of the burned area while 14838 forest fire have burned the 25% of this area [ref.1]

Location	Start time	Duration	Burned area
Bages-Berguedà	04/08/94	4 days	46.000 ha
Gualba	10/08/94	5 days	11.000 ha
Solsonès	18/07/98	3 days	27.000 ha
La Jonquera	22/07/12	2 days	13.000 ha

Table 2.2.7.1: Largest forest fires in Catalonia.

This is a critical information as well as the knowledge of the area affected because it provides the spatial accuracy of the SEVIRI. Real detailed information from the ground gives hints about how the SEVIRI data represents burned areas, unburned enclaves of lands, the approximation location of

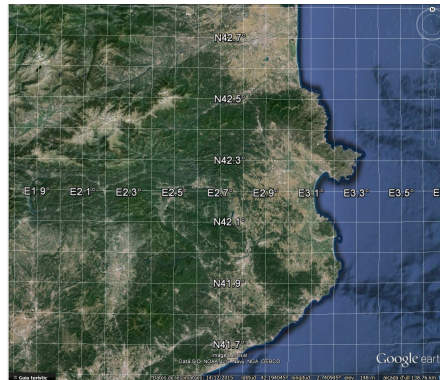


Illustration 2.2.7.2: Longitude and latitude of LaJonquera fire.

the fire, etc,... and of course if the validity of a positive fire alarm. The illustration 2.2.7.1 is used to be compared with one with the detected. This data is focused to an area near the French-Spanish border that reaches the Mediterranean sea. The SEVIRI data also include the coordinates of the each of the radiometric pixels. It important to notice later with the UAV analysis and the manned airplane analysis because the data that is measured and transmitted by SEVIRI -like all space-borne instruments- is periodic and sweeps the same area¹⁶ over a certain period of time.

¹⁶ Orbits are usually described by the number of orbits they perform and number of time until the nadir reaches the same point. Nevertheless, there is the need for small correction a certain time.



Illustration 2.2.7.3: Satellite image of the fires from NASA

The illustration 2.2.7.3 displays the plum of smoke coming from the fire. Later on, studying the nature of fire, the smoke will be described. The large plum of smoke plays a role in some visual channels and also have affect the temperature near the fire. The last illustration also provides the direction of the fire. The presence of clouds is also critical because the visual channel is affected by how the light is reflected in the upper side of the clouds. What affects the visual channels are the clouds and the smoke so the smoke is an indicative sign of fire and the direction of the wind but clouds can mislead the detection of fire.

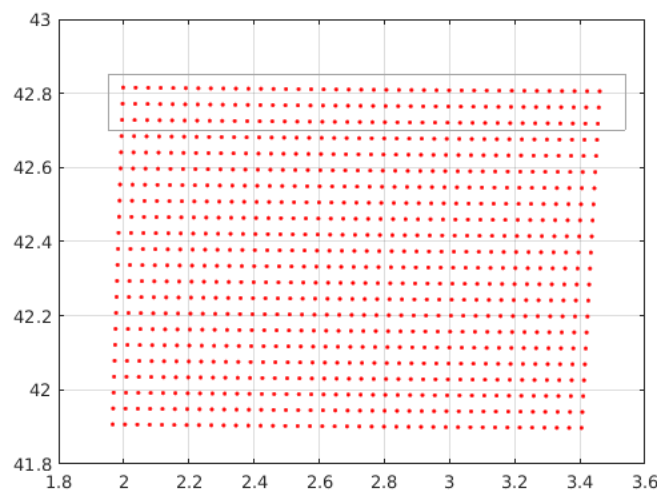


Illustration 2.2.7.4: Areas (with a point in its center) measured by the SEVIRI radiometer.

Each red point on the illustration 2.2.7.4 represents a square -or a rhomboid- with an approximate area of 25km². The data comes from the area of the illustration 2.2.7.4 represents each angular step performed by the radiometer. It comprises a large area but each pixel is like a giant 5x5 km square area. The “image” delivered by SEVIRI are columns and rows of brightness temperature measurements written in georeferenced file with netCDF format and with a .nc extension by longitude and latitude files of the same type, format and extension.

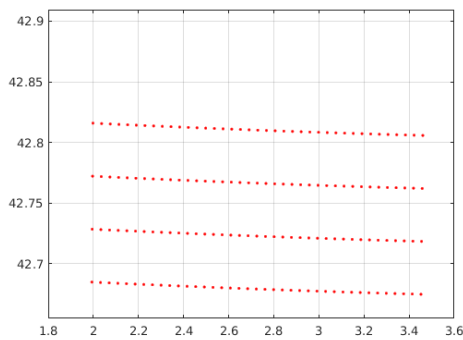


Illustration 2.2.7.6: Rotation error and skew.

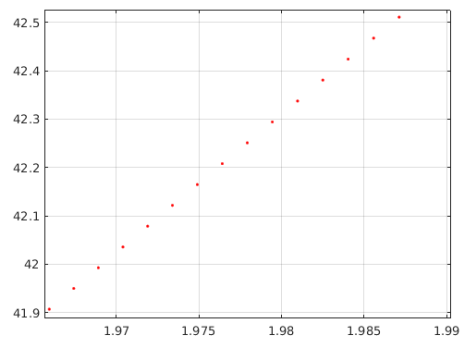


Illustration 2.2.7.5: Rotation error and skew.

The illustration 2.2.7.6 and 2.2.7.5 show that the rows and columns do not share latitude nor longitude; this displacement is caused by the Earth's rotation to the East.

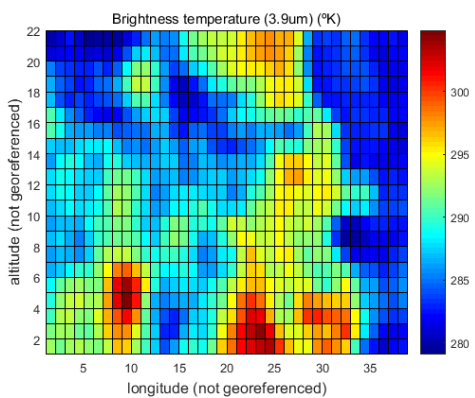


Illustration 2.2.7.7: Raster for brightness temperature (3.9um), instant before the fire.

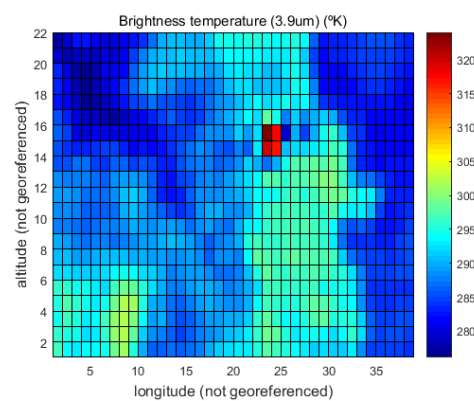


Illustration 2.2.7.8: Raster for brightness temperature (3.9um), instant after the ignition.

This two consecutive rasters of data gives a glimpse about how much the temperature changes

during 15 minutes -before and after the ignition of the wildfire-. They have low temporal and spacial resolution but they are consistent with the temperature: at night during summer sea water is warmer than land because it retains the warm. Land surface is cooler because the lack of sun light during all the night and the lack of thermal inertia. In the illustrations, the sea keeps its temperature while the land changes easy the temperature mainly because of the sun movements. These rasters also show the moment of the ignition of the forest fire. With these rasters and the geolocation files, the brightness temperature is extrapolated to all points with a “cubic” extrapolation of the data.

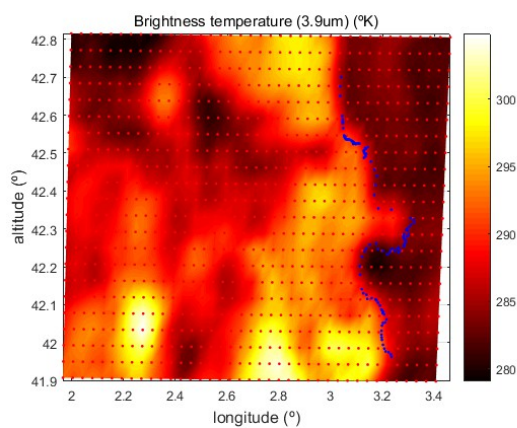


Illustration 2.2.7.10: Instant just before the beginning of the fire (10:45 22/07/2012).

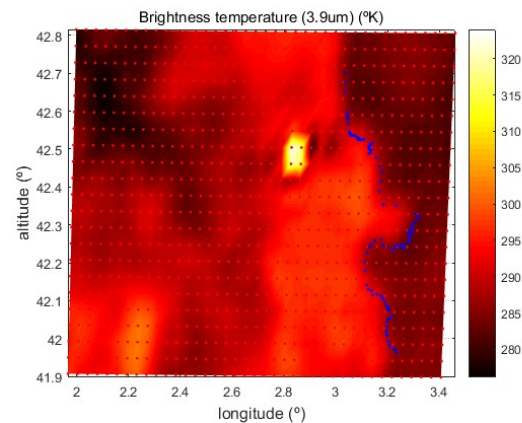


Illustration 2.2.7.9: Beginning of the fire (11:00 22/07/2012).

Illustrations 2.2.7.10 and 2.2.7.9 show information from the SEVIRI, but it doesn't give information about terrain, coast lines, or, of course, the sources of heat. The elevation above the sea, the sun path the sea water explain the source of heat.

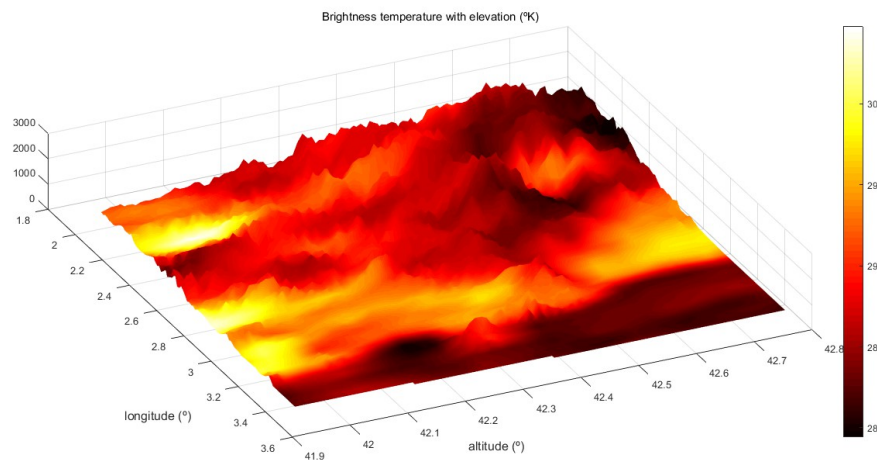


Illustration 2.2.7.11: IR 3.9 um brightness temperature with elevation (10:45 22/07/2012).

The illustration 2.2.7.11 explains why some locations are hotter than others. The flat parts, the plains receive the heat of the sun for more time that other parts. The Northern Western side of the mountains are cooler because of the shadow projected and the time of solar radiation they have been exposed since the dawn.

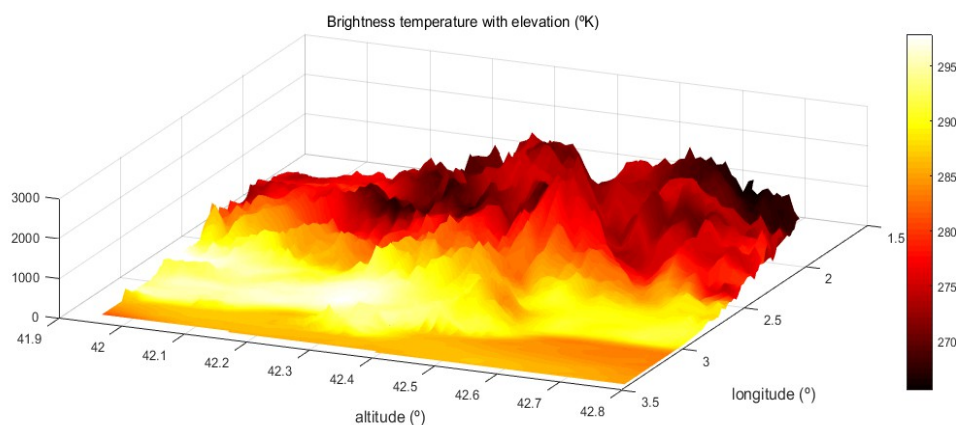


Illustration 2.2.7.12: Brightness temperature (ir 3.9 um) at dawn (08:30 22/07/2012) with elevation (meters).

The illustration 2.2.7.12 shows the IR3.9μm radiation at the dawn (08:30) over the terrain. At that hour only the Eastern side of the mountains is being heated, while the Western side remains at the

shadows.

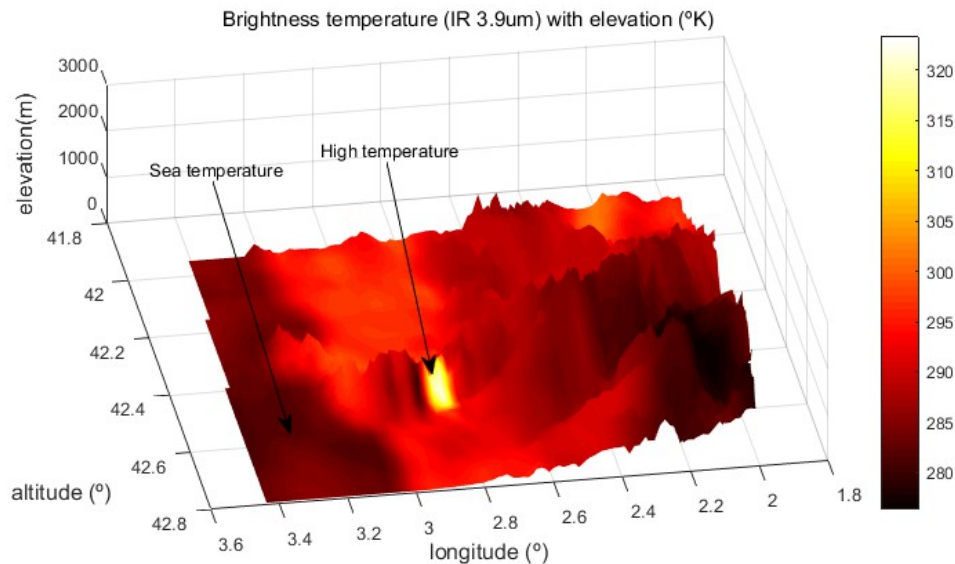


Illustration 2.2.7.13: Brightness temperature (ir 3.9 um) at dawn (11:00 22/07/2012) with elevation (meters).

Even at day light during the summer, some pixels are clearly outstanding among the other hot pixels. And these hot pixels denies the theory that the hottest pixels trigger the fire -and not another event like arson or negligence-. As it is shown in the illustration 2.2.7.12 -flat map- and now the illustration 2.2.7.13, the 4 pixels on fire¹⁷ represent an area of little less than 100km². SEVIRI is able to detect a fire of 2200m² at the temperature of 450°K. However, the illustration 2.2.7.13 do not show the temperature of an area or the fire. The temperature of the flame which has wood as fuel is more than 500°C or 773°K. The brightness temperature for these hot pixels is 320°K or 47°C. The average temperature for the cold or temperate pixels is 300°K or 27°C. There is no way that an area of more than 50km² burns in less than 15 minutes with a flame that is colder than 500°C. The only possibility is that the perimeter of the high intensity fire -or the fire's frontline- overlaps several regions -later pixels- analysed by the SEVIRI.

¹⁷ This is a confirmed fire, not a false positive alarm.

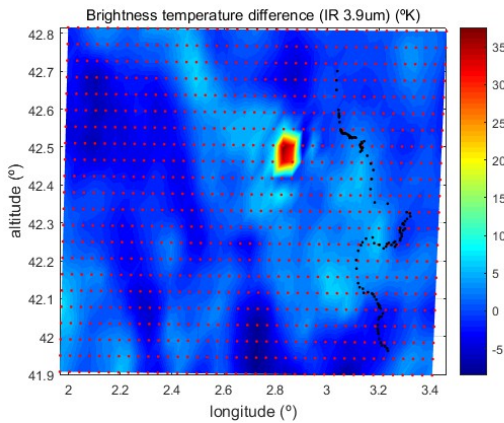


Illustration 2.2.7.14: Brightness temperature difference (IR 3.9um) before and after the beginning of fire.

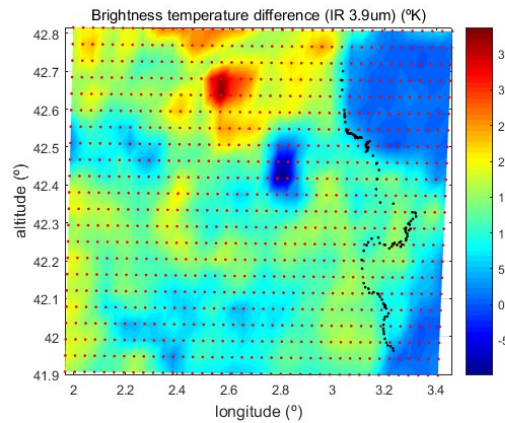


Illustration 2.2.7.15: Brightness temperature difference (IR 3.9um) between 05:00 and 15:00.

The illustration 2.2.7.14 displays the brightness temperature difference between the instant (July the 22nd) before the ignition and the instant after it. Such large difference might be trigger by the ignition of a fire enough large or intense. However, the presence of a large difference of brightness temperature doesn't necessarily mean a forest fire. Some places have a large range of brightness temperature from time to time. In the illustration 2.2.7.15, there is a spot where the temperature raises also 40°K but it doesn't represent an actual forest fire. The span of time is much larger but it doesn't deny the possibility of positive fire alarm.

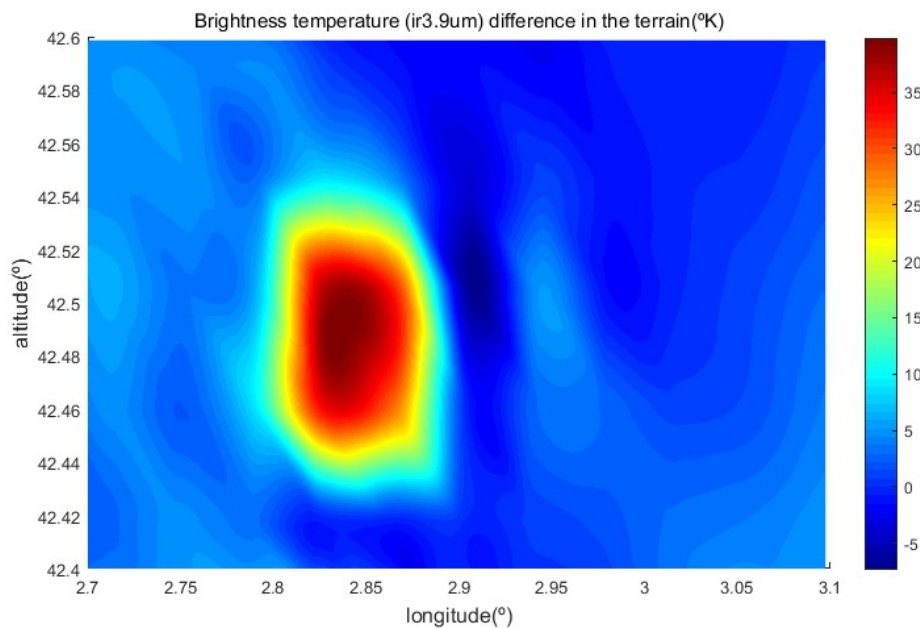


Illustration 2.2.7.16: Difference in brightness temperature between before and after the ignition (10:45 22/07/2012 - 11:00 22/07/2012).

What should be noticed is the drop in temperature around the fires as the time goes on. In less than 15 minutes a zone next to the fire becomes cooler. There is a decrease of more than 5°K. This is a decrease of more than 5°K in spite of the sun is rising and the temperature is becoming warmer anywhere else. Three hypothesis¹⁸ could explain that drop in temperatures:

1. Burned areas: As the forest fire advances, the temperature decreases after the combustion.
2. Shadow of the plum: The smoke that rises from the forest fire creates a shadow that decrease the temperature of a previously illuminated area by the sun.
3. Convective wind: When the heated air rises by the change of density, it pulls cold air from below.

¹⁸ These are hypothesis that do not appear in the bibliography.

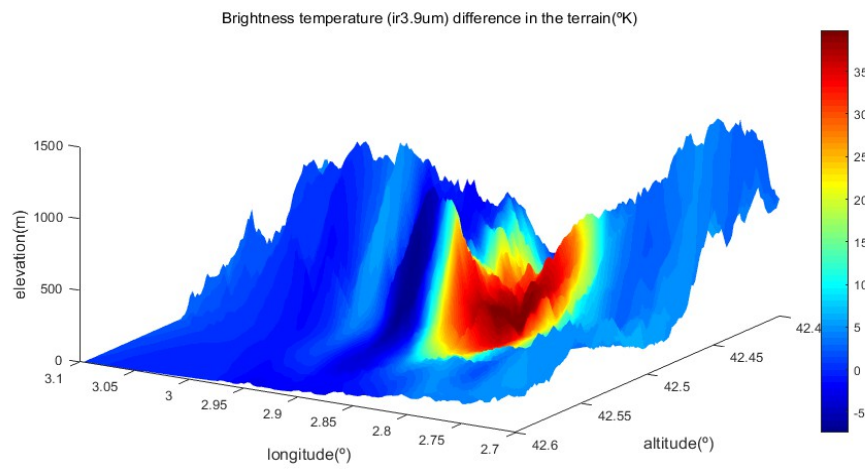


Illustration 2.2.7.17: Difference in brightness temperature between before and after the ignition (10:45 22/07/2012 - 11:00 22/07/2012).

The illustration 2.2.7.17 discards the convection wind and the burned area hypothesis. The shadow is caused by the sun and the plum of smoke. At 11:00 on July the sun is at its highest position with a small inclination to the South.

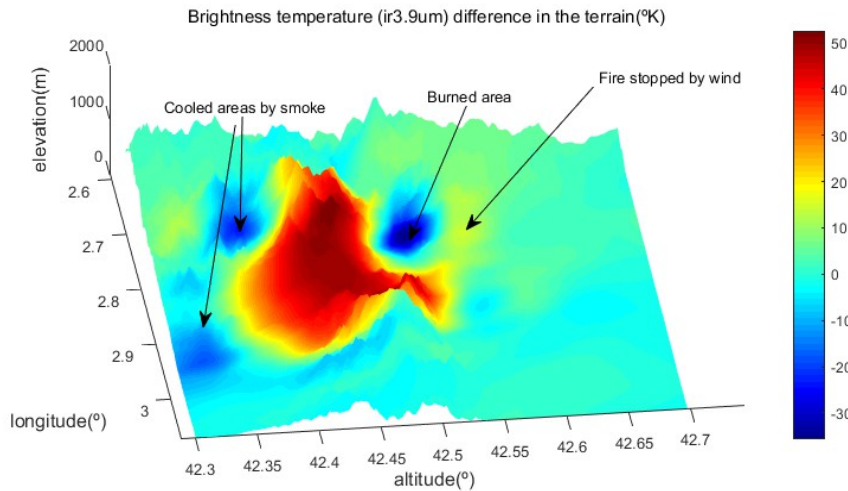


Illustration 2.2.7.18: Difference in brightness temperature between before and after the ignition (10:45 22/07/2012 - 14:00 22/07/2012).

In the illustration 2.2.7.18, after 3 hours the propagation of the fire and smoke becomes obvious. Despite of that the day is becoming warmer some flat zones are becoming colder next to growing hotter fire. The reasoning behind it is that the plums of smoke are hiding the sun radiation to the ground. In conclusion, the smoke do not emit noise equivalent power at the wavelength of $3.9\mu\text{m}$.

Another channel that measures the Earth's surface temperature is the channel 9 that analyses the $10.8\mu\text{m}$ wavelength brightness temperature. This one also analyses the temperatures but its sensibility is lower to the $3.9\mu\text{m}$ channel. In the algorithms used -the thresholding contextual and the thresholding multitemporal algorithms- is combined with the channel 4 ($\text{IR}3.9\mu\text{m}$). Provided that the $3.9\mu\text{m}$ channel has a higher sensibility than the $10.8\mu\text{m}$ channel, their difference between the channel 4 ($\text{IR}3.9$) and the channel 9 ($\text{IR}10.8$) will reveal how the temperature progress. Another particularity of the channel 9 is its linearity with the temperature. The channel 4 certainly has a great sensibility with the changes of temperature but it is not as lineal as the channel 9.

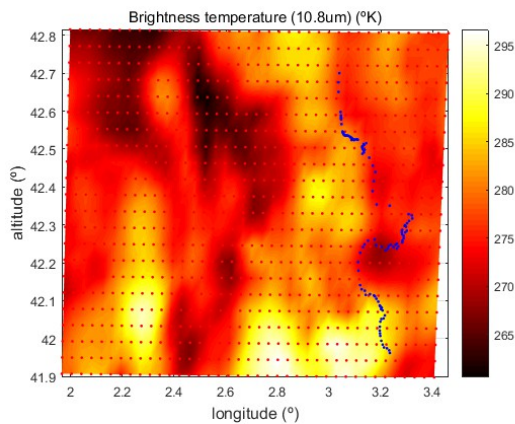


Illustration 2.2.7.19: Brightness temperature before the ignition of the fire (10:45 22/07/2012).

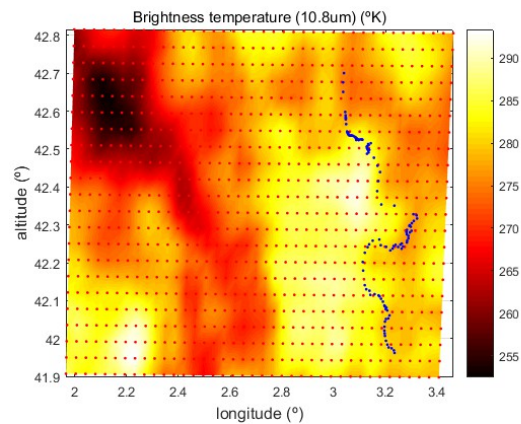


Illustration 2.2.7.20: Brightness temperature after the ignition of the fire (11:00 22/07/2012).

The illustrations 2.2.7.19 and 2.2.7.20 prove how little the change before and after the ignition because of the low sensibility of the channel 9 (10.8 μ m). The range of temperature is also narrow. The window associated to this wavelength might be more attenuated by water vapour.

The next channel analyzed is the IR13.4 μ m channel -or channel 11-. The bandwidth of this channel is absorbed by the carbon dioxide (CO₂) and water vapour (H₂O). The SEVIRI instrument is also designed to determine radiances needed to calculate the CO₂ profiles of the atmosphere from the surface to the stratosphere. The forest fires emit vapour and CO₂ gas but also other gases like carbon methane (CH₄), nitrous oxide (N₂O)), photochemically reactive compounds (e.g., carbon monoxide (CO), nitrogen oxides (NO_x), etc... CO₂ emissions might not indicate the exact location of the fire but it could provide information about the whereabouts of the fire. The channel 11 is used to measure the brightness temperature coming from the CO₂ but it doesn't give information about the exact location of the fire.

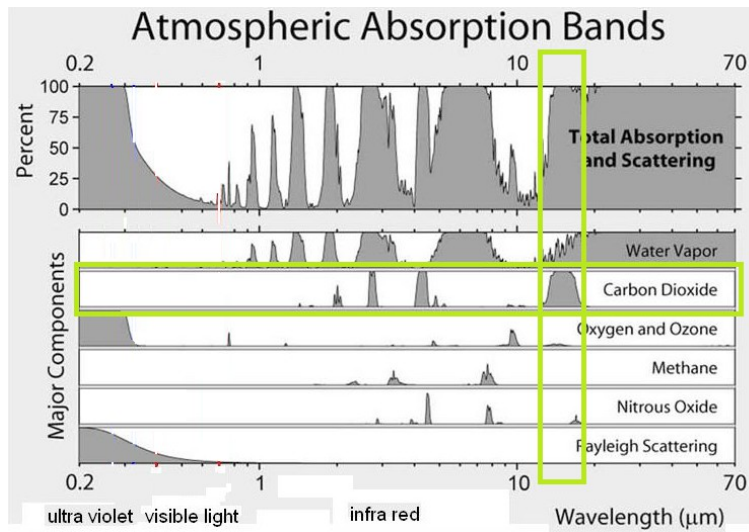


Illustration 2.2.7.21: Atmospheric absorption bands (Carbon Dioxide highlighted).

As it is shown in the illustration 2.2.7.21, the channel's bandwidth from 12,40μm to 14,40μm overlaps with the Carbon Dioxide absorption and also the water vapour absorption. However, there is the need to prove and confirm that the emissions from wildfire are able to detected and tracked because once gas are recognized and its direction, the propagation of fire by wind can be guessed.

The visual channel only works under a range of sun illumination. The visual channels 01, 02, 03 inform about reflection of sun radiation [ref.7].

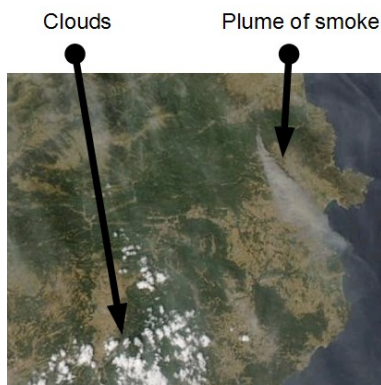


Illustration 2.2.7.22: Satellite high resolution image of 2012 North Catalonia forest fire.

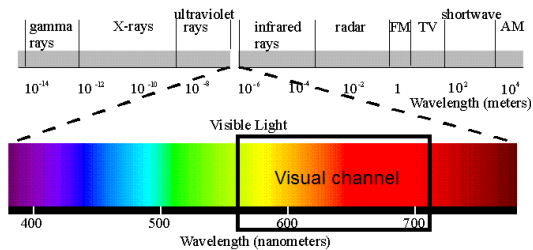


Illustration 2.2.7.23: Visual light inside the channel 006.

This visual channel is unable to discern all colors, hue, tonalities, saturation, etc, It has the ability to

measure the reflection inside its bandwidth. It measures the intensity of sun radiance with wavelengths from $0.56\mu\text{m}$ to $0.71\mu\text{m}$ as it is shown in illustration 2.2.7.23. The white color or the gray color of the smoke are also inside these visual wavelengths. As it can be seen in the illustration 2.2.7.22, the visual intensity of the luminosity coming from the smoke is different to the one coming from the Earth surface. So if the soil have a different luminosity, then the channel detects the changes in the luminosity or brightness. However, the uncertain movement of clouds are also detected as a change of luminosity over time, and there is a periodical change of luminosity because of the shadows created by the terrain (mountains, valleys,...).

The visual change of luminosity caused by the smoke is another way to detect the forest fire; but it has a important disadvantage: there is a critical delay between the ignition and time the plume of smoke is large enough to be notice by the radiometer.

Channel number	Spectral band (μm)	Characteristics of Spectral Band (μm)			Main observational application
		λ_{cen}	λ_{min}	λ_{max}	
1	VIS0.6 (Visual)	$0.635\mu\text{m}$	$0.56\mu\text{m}$	$0.71\mu\text{m}$	Surface, clouds, wind fields
2	VIS0.8 (Visual)	$0.81\mu\text{m}$	$0.74\mu\text{m}$	$0.88\mu\text{m}$	Surface, clouds, wind fields
12	HRV (High Resolution Visual)	Broadband (about $0.4 - 1.1\mu\text{m}$)			Surface, clouds

Table 2.2.7.2: Visual channels in SEVIRI.

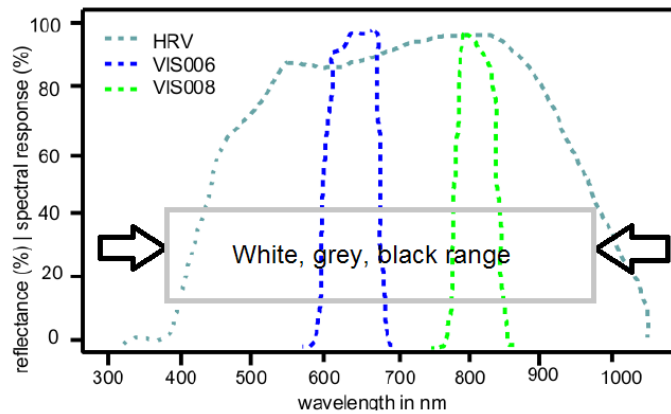


Illustration 2.2.7.24: SEVIRI visual response for HRV, VIS006 and VIS008.

The grey, white color is achromatic and in that case no color (frequency) prevails. If all the visual data is available, it is possible to determinate the color of the area analyzed. Knowing that clouds and smoke from forest fire are achromatic -white, gray, black scale-, it is possible to discern them from the earth's surface if the illumination from the different visual channel describe a gray scale color.

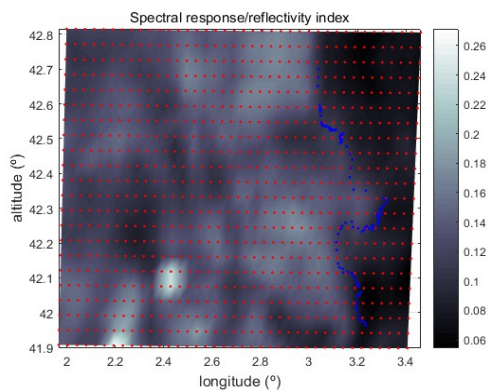


Illustration 2.2.7.25: Reflectivity index before the beginning of the fire (vis006).

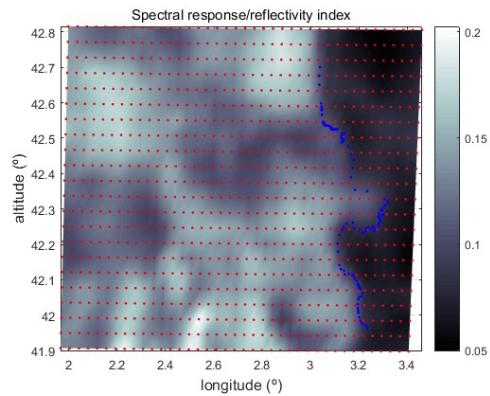


Illustration 2.2.7.26: Reflectivity index after the beginning of the fire (vis006).

These two pictures (2.2.7.25 and 2.2.7.26) represent the reflectance. The radiance emitted by the sun is reflected by the atmosphere or the earth's surface. There are outstanding spots of brightness that are cause by white visible clouds. The different visual channels are able to detect snow on the

Earth's surface, snow clouds, water clouds and sea water depending on the reflectance of these channels. The ability to detect clouds have many purposes for any fire detection application. The first ability of these channels is the detection of plumes of smoke. The second feature is to detect during cold clouds that hide or distort the temperature from other channels that provide other channels like the important channel 4 and less critical channel 9.

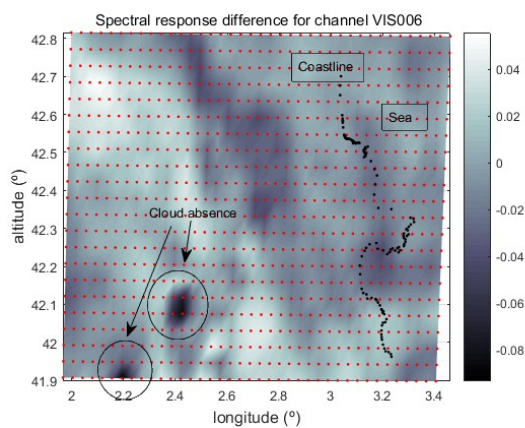


Illustration 2.2.7.27: Spectral response difference in 15min (10:45 22/07/2012 - 11:00 22/07/2012).

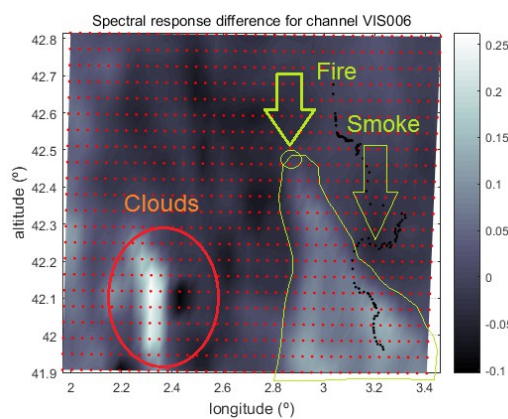


Illustration 2.2.7.28: Spectral response difference in 4 hours (10:45 22/07/2012 - 14:45 22/07/2012).

As the time increases from the ignition, the plume of smoke from the initial place becomes more and more visible and clear as long as there is enough sun light; but the time required to make it visible is more than 4 hours under sun light and be able to distinguish it from . It provides information about the speed and direction of wind. However, it cannot be included as a part of a near real time system because of all the conditions and the time required to reach a conclusion. The shadow of smoke just lowers the temperature near the place where the fire is taking place. The reason behind it is the movement of the sun and the altitude of the plume. That fact makes the detection of the cooled areas by the smoke impossible.

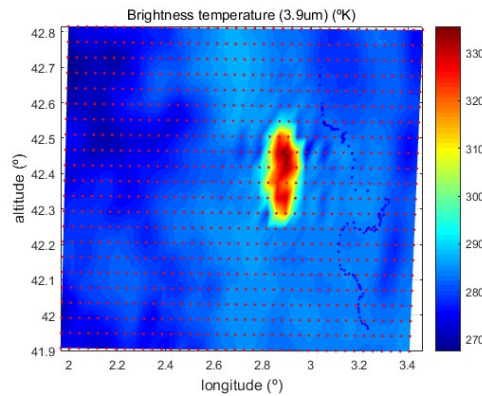


Illustration 2.2.7.29: Brightness temperature (3.9um) after 9 hours (19:15 22/07/2012).

The illustration 2.2.7.29 denies the fact that plume of smoke decreases the temperature wherever it moves. There is no trace or hint of lower temperatures near the plume of smoke when this is far away of the flames despite in the visual channel is possible to the plumes of smoke. Nonetheless, the plumes of smoke lower the brightness temperature near the zone of the fire.

2.2.8. Thresholding Contextual algorithms applied

The contextual algorithms just use the data of one instant over the terrains to detect the fire. There are more than one contextual algorithms. All are utterly based on the ability of the IR 3.9 μm channel to detect a change of temperature. They also use the channel 9 (IR10.8 μm) -or the difference between -

$$T_{3.9\mu\text{m}} > \mu_{3.9\mu\text{m}} + f \cdot \sigma_{3.9\mu\text{m}}$$

$$T_{3.9\mu\text{m}} - T_{10.8\mu\text{m}} > \mu_{dif} + f \cdot \sigma_{dif}$$

Text 2.2.8.1: Last equations for thresholding contextual algorithms.

The μ (average or mean) and the σ (standard deviation) are calculated from a NxN matrix. It check all the pixels inside all the possible NxN matrix¹⁹. The matrix must comprise the readings of an area

¹⁹ All matrix imply square NxN matrix of contiguous readings or pixels.

big enough to have the same temperature while its fire represents a small fraction of pixels.

$$T_{3.9\mu m} - T_{3.9\mu m nbmin} > 15^\circ\text{K}$$

$$T_{3.9\mu m} > 315^\circ\text{K}$$

$$T_{3.9\mu m} - T_{13.4\mu m} > 40^\circ\text{K}$$

$$VIS006 \leq 0.15$$

Text 2.2.8.2: Other equations for thresholding contextual algorithms.

Where

$T_{3.9\mu m nbmin}$ is the neighbouring minimum brightness temperature,

VIS006 is the visual solar channel for the wavelength 0.6 μm .

$T_{13.4\mu m}$ is the brightness temperature from the CO_2 .

The conditions described in the equations 2.2.8.2 are another type of contextual algorithm as it does use data from that very instant. Like the first contextual algorithms it compares two or more contiguous pixels and validates fire if the difference in brightness temperature is large enough. The reason for a condition that implies the channel 1 (0.6 μm) is based on the fact that this channel measures the sun radiation reflectance[ref.7]. A low reflection of sun radiation implies that the heat comes from the fire and not from the sun.

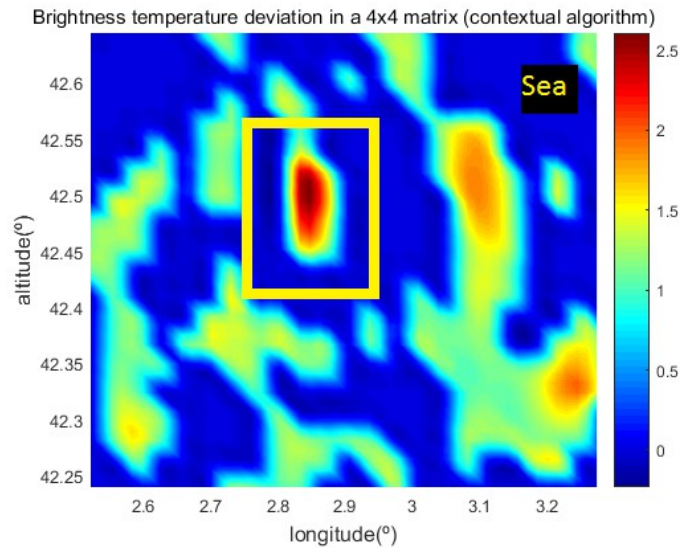


Illustration 2.2.8.1: Brightness temperature standard deviation at the beginning of the LaJonquera forest fire.

The illustration 2.2.8.1 shows the relation between the brightness temperature of one pixel and the deviation of the matrix where this pixel belongs to. What the thresholding contextual algorithm does is establish a threshold that indicates whether and how much there is an anomaly in temperature inside a matrix with other brightness temperature pixels.

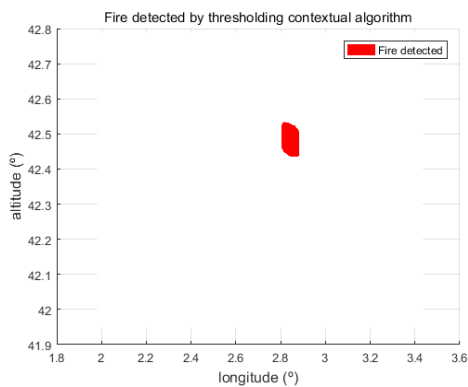


Illustration 2.2.8.2: Fire detect by thresholding contextual algorithm (11:00 22/07/2012).

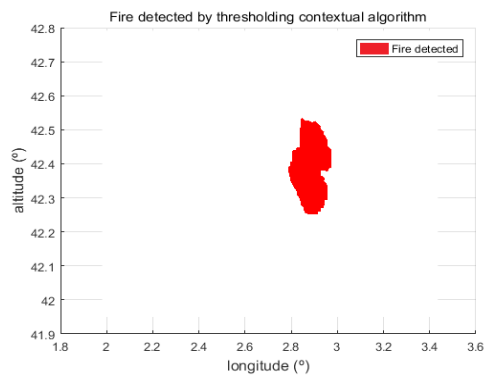


Illustration 2.2.8.3: Fire detected by thresholding contextual algorithm (20:00 22/07/2012).

In the illustration 2.2.8.2, the detection of fire does match with the confirmed fire at the very beginning of it -less that 15 minutes after the ignition-.The illustration 2.2.8.3 shows the same fire grown after 9 hours later but this algorithm fails to detect another fire in the town of Portbou that was ignited at the 19:00 of the same day.

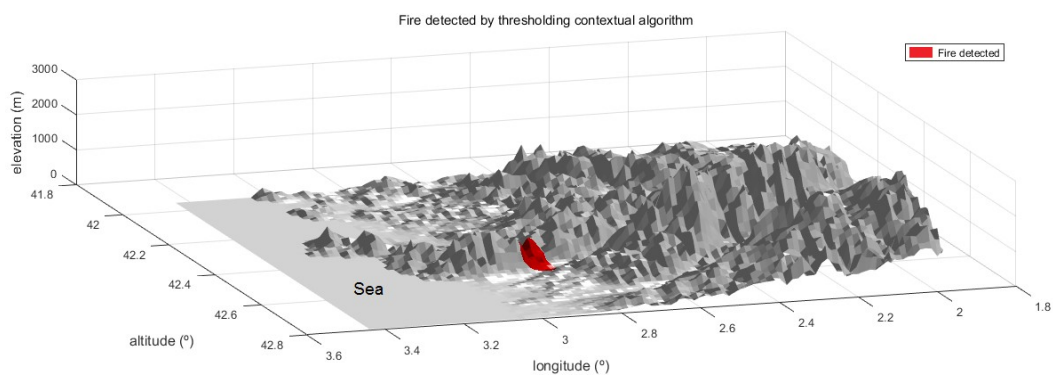


Illustration 2.2.8.4: Fire detect by thresholding contextual algorithm over the terrain (11:00 22/07/2012).

In order to visualize better the fire, elevation is added so that the location of ignition is known. The detected area in the illustration 2.2.8.4 matches the location where the fire begins. However, the area detect is, in fact, large and contains errors of north-south and west-east alignment. The geometric accuracy specifications for SEVIRI Level 1.5 data from Meteosat-8, Meteosat-9 and Meteosat-10 are less 3.0 km or, in other words, their absolute error is less than one pixel [ref.6].

Limitation of contextual algorithms

After applying the contextual algorithms, several problems are observed. Despite it detects the fire without a history of data behind it, the first limitation is the fact that all the matrix analysis implies a long process to determine if there is a pixel of fire or not. It requires the calculation and comparison of all possible square contiguous matrix with all their pixels. The second limitation is the assumption that the temperature changes gradually slow along the terrain. When there is a sudden change of temperature in half -for example- the pixels in the matrix, the standard deviation of the matrix becomes very high (see equation 2.2.8.2). This high deviation hides possible fires.

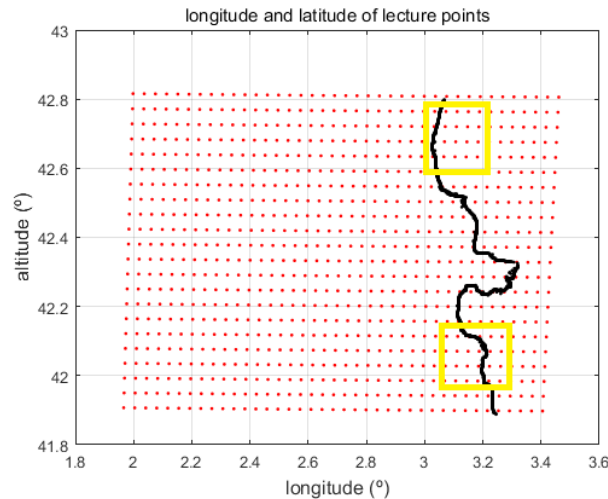


Illustration 2.2.8.5: 2 NxN matrix in a sudden change of temperature.

The illustration 2.2.8.5 shows the two cases that might result in errors. In the upper square of this illustration, the matrix has a very low standard deviation (σ) because almost all the pixels *2 are from the sea which always have the same temperature. Water maintains its temperature and it doesn't have any elevation or irregularity in the “terrain”. When the matrix has a few of warmer spots it is detected as a contextual anomaly and a fire pixel. On the contrary, in the lower square, the matrix has a high standard deviation because of the sudden change of temperature among many of its pixels. This deviation will hide possible pixels on fire near the coast.

2.2.9. Thresholding Multi-temporal algorithms applied

As its name states, this method uses information from recorded brightness temperature about the location analysed. On a daily basis, the temperature profiles repeats and when there is an unexpected sudden increase of temperatures, a forest fire is assumed.

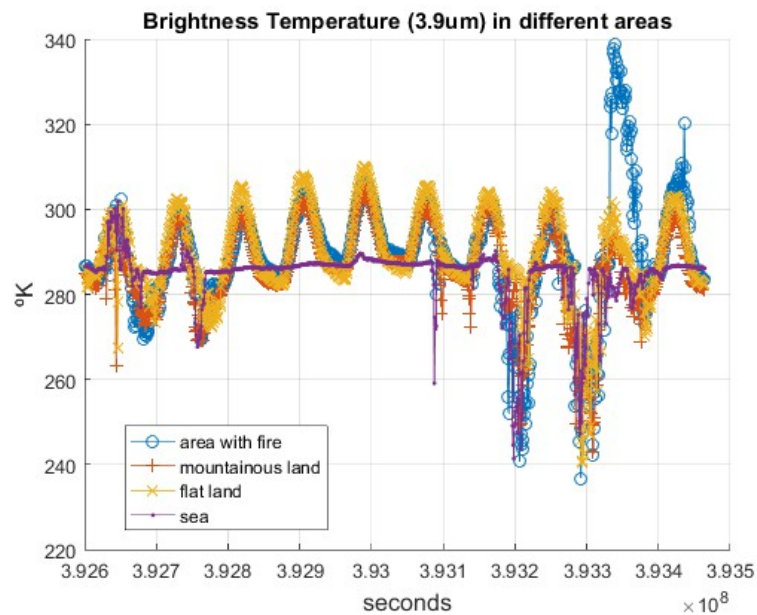


Illustration 2.2.9.1: Brightness temperature of 4 different points during 10 days.

The illustration 2.2.9.1 shows the brightness temperature of four points. The temperature curves based on points located on the land follow the same periodic patterns. The sea temperature do not oscillate because of the large water's thermal inertia. The area with fire does not follow this pattern but suffers the decrease of temperature because of the night.

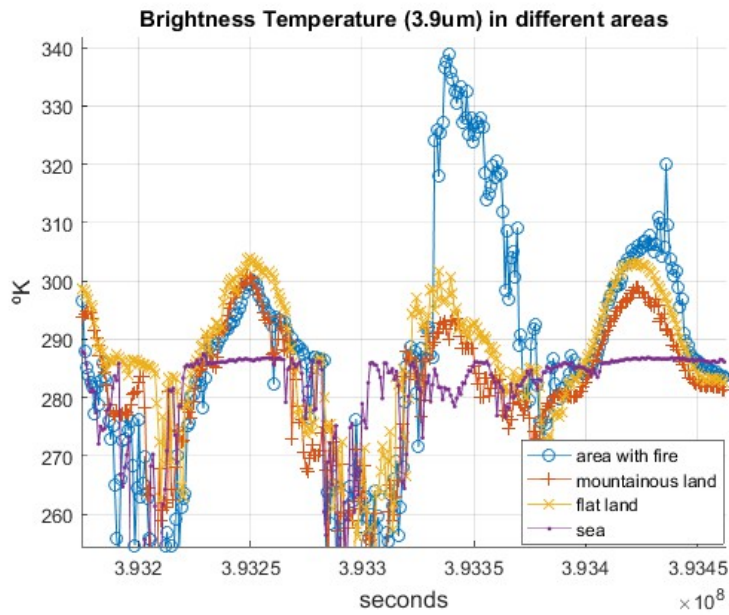


Illustration 2.2.9.2: Channel 4 (IR3.9) during in 4 points during the fire.

The illustration 2.2.9.2 observes the exact time of the fire. In order to detect the forest fire in its early stages until the last vestiges of it, there must be an accurate threshold at every hour. There are, however, many points which suffer a sudden decrease of temperature as if something is attenuating the brightness temperature. The sea -as well as the other areas in land- usually doesn't have sudden changes in temperature. Fortunately, the vast majority of all unreal changes are sudden decreases. These changes are caused by cold clouds. The fast decreases of brightness temperature belong to invisible cirrus that cannot be detected by visible channels.

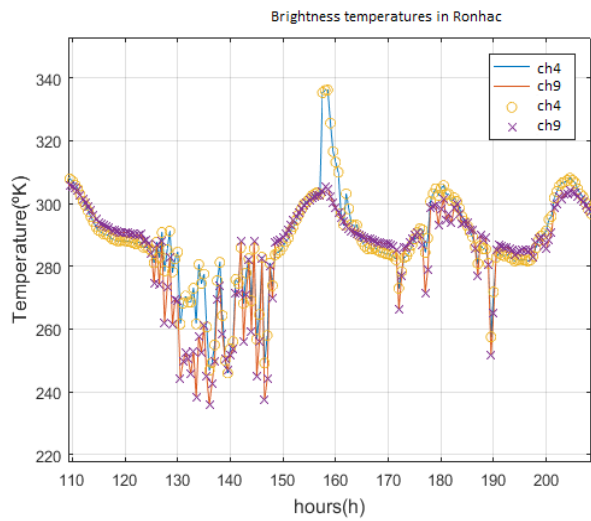


Illustration 2.2.9.4: Brightness temperatures in a fire spot in Ronhac (Marseilles, France).

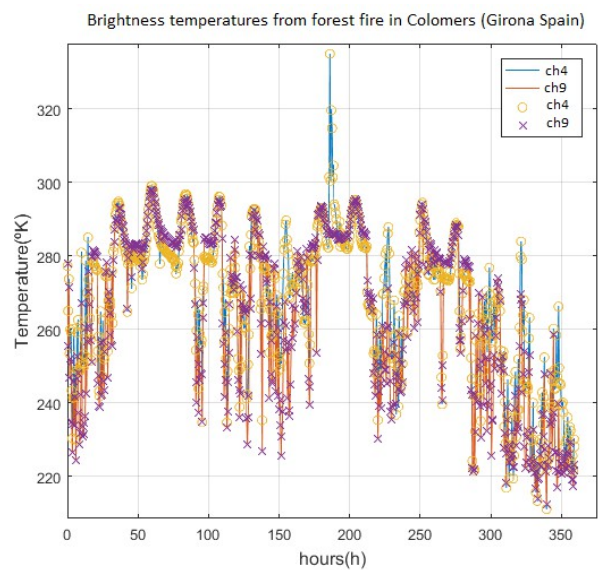


Illustration 2.2.9.3: Brightness temperatures in a fire spot in Colomers (Girona, Spain).

The temperature (illustration 2.2.9.4) from other forest fires displays the same fast decrements caused by cold clouds. This clouds cannot be detected by their reflectivity with the visual channels 1, 2 or 3. In the case of the Colomers²⁰ forest fire -in the illustration 2.2.9.3-, the presences of this phenomena is very abundant. The difference of sudden decrements might be linked to the fact that the Colomers forest fire occurs during winter²¹, therefore, explaining the presence of invisible cold winter clouds in the atmosphere that mask the brightness temperature from the ground. However, the fact that this high-altitude invisible cold cloud is invisible could be proven helpful. The channel 11 (IR13.4 μm) is unable to detect the smoke but this smoke from the forest fire can be see from a visual channels. The measured reflectance channels 1, 2, 3 not only is able to detect changes in the visual spectrum but also some information about the color of the smoke. It is possible to notice in the illustration 2.2.9.5 how there is a change in the visual channel during the time of the forest fire. The change in the reflectance must be caused by a moving cloud or by the plumes of smoke. In the chapter 2.4., it is proven that the smoke color -or a wide range of grays- have the same reflectance for a wide bandwidth. In the illustration 2.2.9.5, the day of the forest fire -inside the green rectangle-, the channels reflectance is very similar making to each other probing that the color is inside the gray range. Other days doesn't have clouds, while other yes.

20 Colomers is a town in the Girona province near Vilopriu. Vilopriu is an infamous town for the frequency of its forest fires. Vilopriu has suffered 32 times in 6 years.

21 This Colomers forest fire occurred at 17:30 on November the 11th 2013.

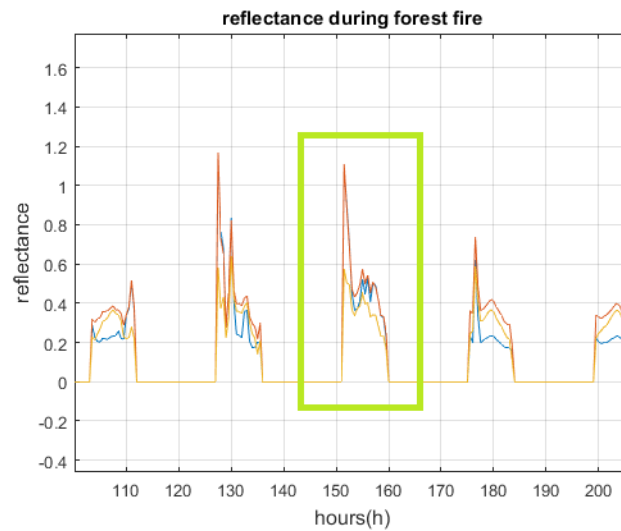


Illustration 2.2.9.5: Reflectance by visual channels during forest fire in Colomers (Girona).

Limitation of contextual algorithms

There are two limitations with this kind of algorithms. The climate and weather keeps changing; one location repeats the increase and decrease during a season, month, week,... that varies inside a certain range. The spacial accuracy of the SEVIRI may play a factor in the algorithms too. The other factor is the cold clouds that cannot be detected by the visible channels. Invisible cold clouds that cause sudden decreases of brightness temperature do not affect the contextual algorithms.

2.3. UAV Analysis

This work develops a system to achieve two main goals the detection and movement prediction and the detection of the hot spots for wild fires or forest fires. However, the project is not limited to this functions, it must be able to follow, track the fires -give them patterns- and count the burned areas. This also must have the ability to "stabilize" the image while the UAV is moving or the

Limitations

There are clear limitations that must be taken into account. There are two main limitations based on the instruments and the place where they are placed. What differentiates the UAV from manned aircraft are the payloads, their sizes and their weight. The UAV's payload should be contained in a 170mmx80mmx80mm rectangular prism and the weight should be lower than 500g. If the UAV is extremely big let's suppose that the payload must weight less than 5kg. The limitations are the geometric errors, trajectory with geometric errors, the resolution and availability provided by the UAV and the SMOS satellite. Fortunately this also limits the data and the imagery this project must deal with.

Usually computer vision programs trace a moving object while the background remains the same even if the point of view moves to some degree. In the current case, this will not be true. The fire and the smoke change the background.

2.3.1. Understanding the stages of the proposed UAV deployments

In order to obtain thermographic and visual imagery that embraces a large area, the drone must reach a certain altitude. The UAV will be plugged to a balloon which will be elevated to a minimal altitude. The drone is expected to reach the range between 10km and 20km of altitude; that's as high as the altitude that commercial airplanes use in the cruise stage of their flights. Before that mentioned altitudes the imagery is not valid or the imagery is too distorted. The elevation and coordinates are measured by a GPS receptor. This deployment has two options regarding how it operates and when it does a "sweeping analysis".

- Balloon-suspended analysis -using the balloon as a lifejacket in the sky-

- Self-propelled analysis -the UAV flights and move by itself above the area of interest-

In the illustration 2.3.1.1, the balloon takes off from the origin point. The origin point and destiny point must be the same in order to recover the hardware and information if this one is not been transmitted while recording the fire from above. The origin point doesn't require a starting point

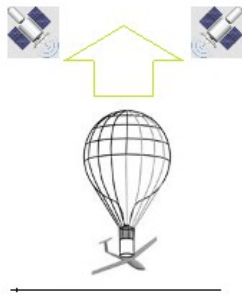


Illustration 2.3.1.1: Take-off from ground.

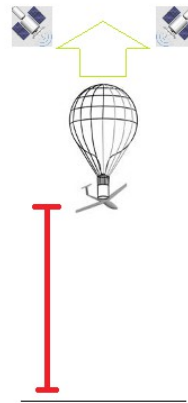


Illustration 2.3.1.2: Gaining altitude (ground too close to analyze).

dangerously close to the fire because the elevation is high enough to record a large area.

Regardless of the weight of the UAV and its payload, the balloon would take several minutes to reach the target elevation. The minimal elevation over the terrain are 10km so it would take some minutes -more than 15 minutes- to reach the ideal elevation. At this point the analysis has not begun. In the illustration 2.3.1.2, the UAV and balloon gain altitude, the altitude is measured by the GPS on board to be able to grasp the elevation of such UAV.

Once it has reach the optimal elevation the analysis begins. The visual and the thermographic -or infrared²² - cameras begin to record the fire -if there is any- and its surroundings. There is the possibility that there is no fire at all but that fact do not change the course of the stages. The lack of fire do not produce a situation that has not been considered. Once the altitude requirement is met, from now on, the deployment chooses one of the operations.

²² The thermographic and the infrared cameras process different wavelengths. Thermographic cameras

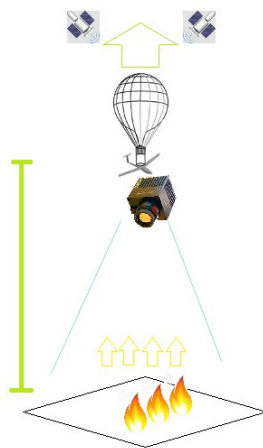


Illustration 2.3.1.3: Optimal elevation reached. Analysis begins.

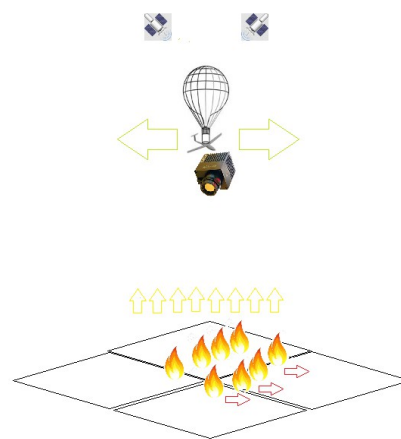


Illustration 2.3.1.4: Recording the ground. Using balloon as lifejacket while analyzing the terrain.

If the UAV (drone) uses the balloon as a lifejacket in the air, the UAV might, or not, propels itself while it is suspended by the balloon in order to correct or change its position. With its payload -a thermographic camera and a visual camera-, the data will be transmitted or stored repeatedly. This is a critical fact because how the data is treated will determine the latency of the system based on drones. Given such a high altitude, the need for movement is little²³ but it cannot be discarded if the wind moves the balloon. The infrared and visual cameras records information as a constant periodic capture²⁴ of pictures that show the forest fire from above.

At certain point, the all process is stopped and the recollection of the data, vehicle and payload begins. After the analysis is decided to be finished the research balloon releases the UAV and it falls by itself.

²³ At 10km, despite any lent or zoom, the camera is able to

²⁴ There is no need for coded video, the fire line speed is doesn't requiere video. Image processing rarely uses video anyway.

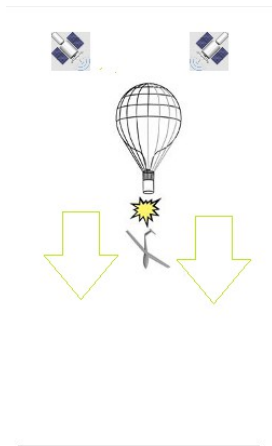


Illustration 2.3.1.5: UAV is unplugged from balloon and begins descend.

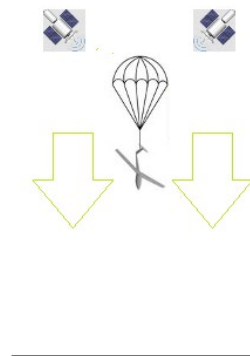


Illustration 2.3.1.6: The UAV descends with a parachute.

After the vehicle has been detached from the -research- balloon (illustration 3.4.1.5), a parachute will open and descend down to a certain altitude. The length of such elevation will depend on the operations that will follow this stage.

If the type of operation include a self-propelled analysis, the UAV will sweep an area instead of just returning to the origin point or take-off. It is unknown how the UAV will patrol, sweep or scan the area. This implies that the analysis must be able to contemplate U turns, all kinds of shifts, a certain velocity, etc,... related to all the possible sweep of the target area.

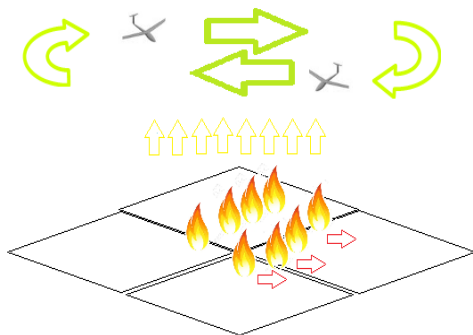


Illustration 2.3.1.7: UAV sweeps the area of interest repeatedly.

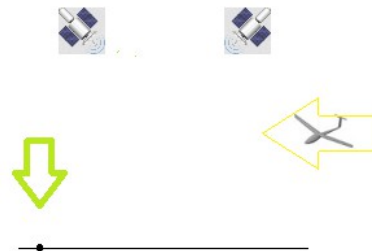


Illustration 2.3.1.8: The UAV returns to the origin point.

The last stage is the recovery of the vehicle and the payload. In that phase the UAV flights by itself self-propelled to the origin point of deployment. And then the data is retrieved if it hasn't be retrieved before.

2.3.2. Unmanned Air Vehicle

The proposed unmanned air vehicle is the Atmos-7 UAV. This UAV has been chosen because of the endurance, range and maximum payload. The fire²⁵ that took place in North Catalonia burned 13,800 hectares or 138 km². That is a sizeable area for the Atmos-7 which has a range of more than 60km. This autonomous vehicle employs autopilot which is ideal for this kind of situations. The UAV is guided by GPS and not by a pilot. The maximum speed of fire spread is between 16 and 20 km/h so the UAV will be left behind.

- Specifications:

- MTOW: 2,9 kg
- Payload: 900 g
- Endurance (payload dependant): 70 to 120 minutes
- Flight modes: Manual and Autonomous
- Take-off: Automatic hand-launch
- Landing Options: Automatic deep stall and/or parachute
- Cruise Speed: 50 to 60 km/h
- Maximum Speed: 105 km/h
- Range: 60+ km
- Wind resistance: up to 30 km/h



Illustration 2.3.2.1: The Atmos-7 UAV system.

Of all the information that is possible to extract from the UAV datasheet, the most critical are the

speeds, altitudes and inclinations, all the factors that influence the flight and therefore the imagery received from the UAV in order to do the tasks related to the wildfire.

2.3.3. UAV imagery errors and distortions:

There will be, of course, distortions and errors coming from the UAV imagery²⁶. There will be systemic errors produced by the cameras themselves and the geometric distortions caused by the unpredictable movement of the camera or produced by the hardware, in other words, geometric and systematic errors.

External geometric errors are usually introduced by phenomena that vary in nature through space and time. The most important external variables that can cause geometric error in remote sensor data are random movements by the aircraft -or spacecraft- at the exact time of data collection, which usually involve: altitude changes, and/or - attitude changes (roll, pitch, and yaw).

The assumption in this work is that the UAV cameras will be able to provide one image each second. The images will be related among themselves, in other words, the imagery will be connected: all images will share parts among themselves despite the speed, roll, pitch... but there will be errors. Despite movements and spins, the code must be able track and quantify the fire and its location on the terrain all the time.

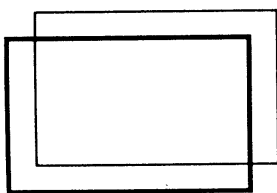


Illustration 2.3.3.1: Shift error.

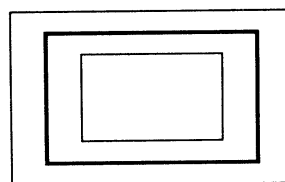


Illustration 2.3.3.2: Scale error.

Shift errors: The UAV and its payload would likely move continuously as they record the terrain and the affected area. The frame which is recorded will change every moment and the designed code must be able to recompose and join in an correct way all the imagery. But the shift error would not only cause by the movements and spins; if there are two or more camera-like devices in large

²⁶ The imagery from the UAV includes still images and video from the visual camera and the infrared -also known as thermographic- camera.

distance they might not match both imagery frames.

Scale error: It is also possible that a fast approximation move or a zoom by one of the cameras might produce fast scale shifts. In other words, the image's frame might include more or less area than the next one. The same phenomena occurs with the two or more cameras: each camera might focus a bigger or a smaller area.

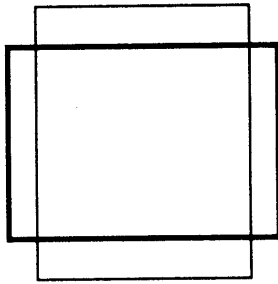


Illustration 2.3.3.3: Vertical/Horizontal error.

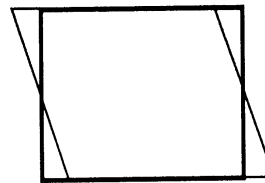


Illustration 2.3.3.4: Skew.

The vertical/horizontal error: There is another kind of error or problem. If the UAV moves fast enough there might be error. The same happens if two or more cameras has different aspects.

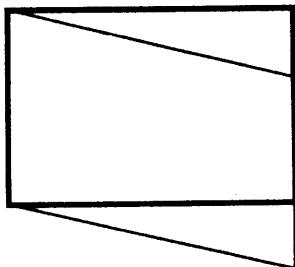


Illustration 2.3.3.6: Skew.

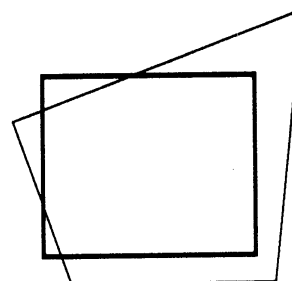


Illustration 2.3.3.5: Projection distortion.

Projection distortion: The area and plane that is being focus might not be exactly perpendicular to the camera focal plane and that fact might produce a projection error.

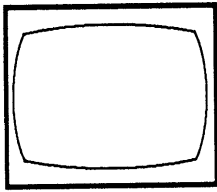


Illustration 2.3.3.7: Earth curvature distortion.

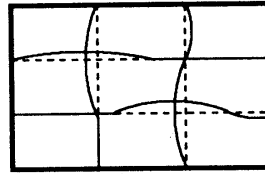


Illustration 2.3.3.8: Terrain relief distortion / displacement.

Distortion due to Earth curvature: That factor might be more important in satellites where the curvature must be taken into account so that the information from the radiometers -for examples- is placed correctly in the coordinates. At the range of elevations between 10km and 20km, this effect must be almost zero but it must be taken into consideration.

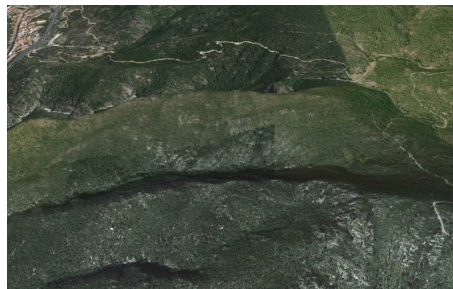


Illustration 2.3.3.9: Example of terrain relief displacement.

Terrain relief displacement: Provided that some terrains are not smooth nor flat, there will be distortions caused by the terrain. So parts of the terrain will be expanded and some others will be compressed by this effect.

2.3.4. Payload Cameras:

The UAV is unable to carry large cameras and, of course, the UAV is unable to carry radiometers. This works takes as payloads and cameras for the UAV the Miricle 110K-25 and the NecF30. The SEVIRI radiometer, for example²⁷, weights more than 260kg. Commercial infrared cameras -because of their small size and much simpler principle and operation- are unable to select or

²⁷ Other example could be radars which require a lot of power and weight much more than a camera.

discern narrow channels unlike space borne radiometers. The SEVIRI radiometer has a better angular resolution which is approximately 125.8 microradians which means 4500 meters but this provides little help for our application which requires much more accurate measurements of burned areas.

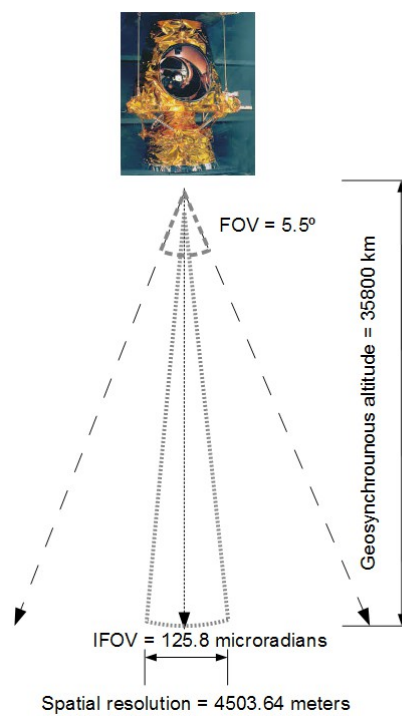


Illustration 2.3.4.1: Radiometer field of vision.

Miricle

The MIRICLE 110K-25 creates 384 x 288²⁸ image in the longwave Infrared (7-14 μ m) band. But what is really important is the size, weight and the resolutions as well as the thermal sensitivity. As it have already mentioned, the SEVIRI radiometer is unable to detect with accuracy the temperature of the fire. The temperature of the fire -or the wood on fire- reaches easily more than 600°C. Although, the SEVIRI is able to detect wildfire when a large area is burned, that fact doesn't show how the fire is distributed or the burned areas.



Illustration 2.3.4.2: Image generated by the thermal imaging camera Miricle.

The Miricle has the thermal sensitivity of less than 60mK at 27°C and it has a spacial resolution of less than 6 meter and a temporal resolution of less than 1 second . That is a perfect combination for the project. With a fully assembled weight of 85 g (without lens) the Miricle 110K-25 is ideal for UAV and field portable applications.

110K-25 (25 μ m pitch)

28 Or a 640x480 pixels resolution.

The New Miricle 110K-25:

- Improved Detection Recognition and Identification ranges
- Super-Sensitivity option
- Low weight (80g 110K-25 XTi)
- Optional low-mass optics .
- FOV = $7.3^\circ \times 5^\circ$
- IFOV = 0.33 mRad

On the other hand, the Miricle camera does not create a visual image simultaneously with the “thermal image”.

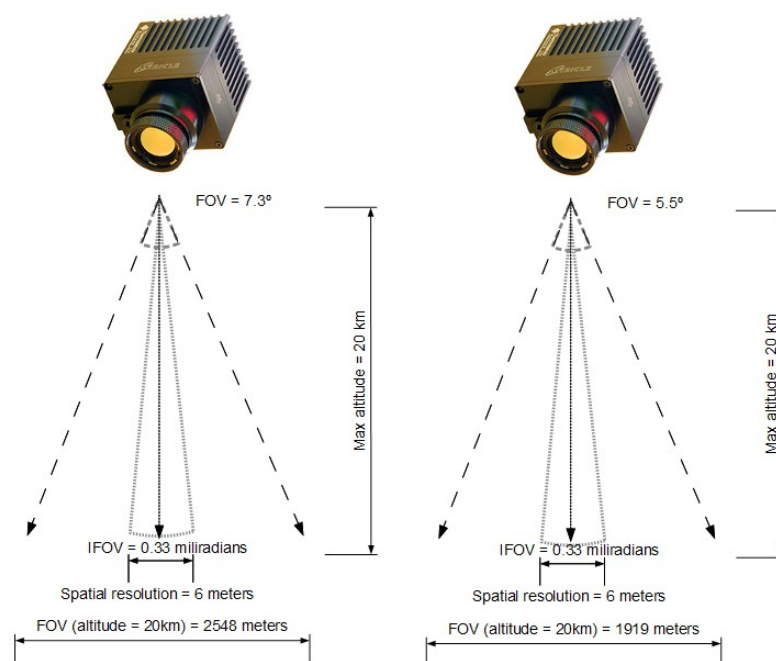


Illustration 2.3.4.3: Spacial resolution and Field Of View at 20km for the Miricle 100k.

NecF30

The Nec is called a fixed-installation Infrared Thermal Imager.



Illustration 2.3.4.4: NEC F30 thermal infrared imaging camera.

Illustration 2.3.4.5: Thermal image from NEC F30.

Illustration 2.3.4.6: Visible image (visual image) from NEC F30.

The NEC F30

The NEC F30 is not as small as the Miricle 110K, and it weights more -about 300 grams-and has more volume than the Miricle 110k. But it has more features than the previous camera, uses the same type of infrared detector and detects a similar wavelength (8-13 μm). The thermal sensivilty is similar, It should be mention that the F30 provide the visual and the infrared image at the same time and with a higher frequency that the Miricle 100k. That's important because it provide matched images, visual images with their infrared counterparts. The Miricle device lack this feature. On the other hand, the F30 has a worse accuracy, its spatial resolution is 60 at the altitude of 20km, fact that might arise problems to detect properly the fire.

- Low weight = 300g
- Optional low-mass optics .
- FOV = 28°x21°
- IFOV = 3.1 mRad

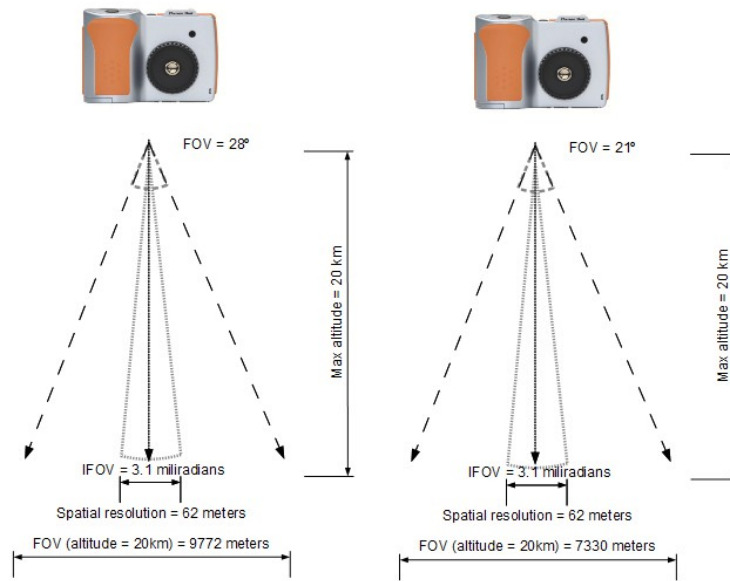


Illustration 2.3.4.7: Spatial resolution and Field Of View for F30.

2.4. Study of the wildfire

The space-borne analysis bases its detection and tracking on the temperature of a certain area²⁹. That area is so large that it just analyse the temperature³⁰. However, an study with another scale and point of view make possible its study by its propagation, shape, colours, speed and size, including temperature itself. The UAV analysis, because of its payload, relative proximity and resolution has the ability to give much more exact information about the fires.

Heat radiation is a phenomenon that a matter has a certain temperature so to radiate electromagnetic wave. The temperature is higher in burning area, the total volume of radiation is much higher so that

²⁹ That area is more than 4 km²

³⁰ Several articles study how the CO₂ absorbs certain wavelengths rendering it use for the use and tracking of wild fires.

combustible matter around would be preheated and dewatered quickly to speed up fire spread.

Heat conduction transfers heat inside a combustible matter, but heat convection and heat radiation transfer heat among different combustible matters. Forest fire could spread around in those three ways and cause large-scale fire hazards.

2.2.2. Terrain: Shanxi province is located on a loess mountainous plateau with a various and complex terrain, which not only influences the type of combustible matters and humidity, but also significantly impacts heat transfer. When the slope is steep, water of combustible matter evaporates quickly, and the combustible matter is prone to ignition vice versa. Besides, the relative position between burned area and unburned area changes with the degree of slopes so to influence the volume of radiated heat and then the velocity of fire spread. In general, with the increase of slope degree, the velocity of fire spread increases, and fire on upward side of slope spreads quickly and the one on downward side of slope spreads slowly.

2.2.3 Wind: Wind speed and wind direction are major factors to influence fire spread. Wind speed can accelerate evaporation of water. Within a certain range, the more intensive is the wind, the faster is the fire spread. The average wind speed varies from 1.4 to 4.5 m/s and the highest wind speed commonly varies from 14 to 20 m/s in Shanxi province. Wind is more intensive in spring than it is in other seasons. Besides, transmission lines usually are laid out at higher ground where wind is more intensive and forest fire spread is influenced significantly. On the other hand, wind direction influences the direction of forest fire spread. Influenced by mainland low pressure, south and south-east wind dominates during summer half year, and affected by Inner Mongolia high pressure, north & north-west wind dominate during winter half year in Shanxi province. Therefore, forest fire spread direction changes with seasons.

2.2.4 Temperature and humidity: Combustible matter's temperature and soil's temperature influence the igniting point, and are indirectly influenced by air temperature so to affect forest fire spread. Meanwhile, air temperature and humidity significantly influence moisture content of combustible matter. The average temperature in Shanxi province varies from 3.7 to 13.8°C. Influenced by horizontal distribution, it is warm in south and cool in north. Influenced by terrain, weather vertically varies obviously. Semi-arid climate dominates in Shanxi province but it is semi-humid climate in a small part of regions with high mountains and in southeastern Shanxi. The special climate condition influences the forest fire spread there.

2.4.1. The shape of fire

The UAV onboard information may not contain fuel moisture, inclination (slope) and terrain information, wind speed and wind direction, type of vegetation but the fire creates a perimeter from a single point of ignition. This perimeter and its growth describe certain patterns. In the illustration 7 shows a large area of forest fire with its own perimeter. Notice that the front-line fire has different thickness.



Illustration 2.4.1.1: Infrared image. Fire describing a perimeter.

There is another interesting fact that has been proven very useful in the UAV analysis. The smoke is transparent to the infrared wavelengths. So the visual camera may give the visible information; the smoke rises because of the heat -convective force-. At 10km of altitude, the UAV observe the smoke, while the smoke doesn't emit radiative heat or infrared wavelengths the infrared from the flames give temperature information and the disposition and location of the flames. There is no fire without smoke so the combination of visual information and infrared information. In the illustration 8, it is possible to see that the smoke coming from the fire. The smoke doesn't hide the fire or at

least all the heat and “light” coming the tree that are being burnt.

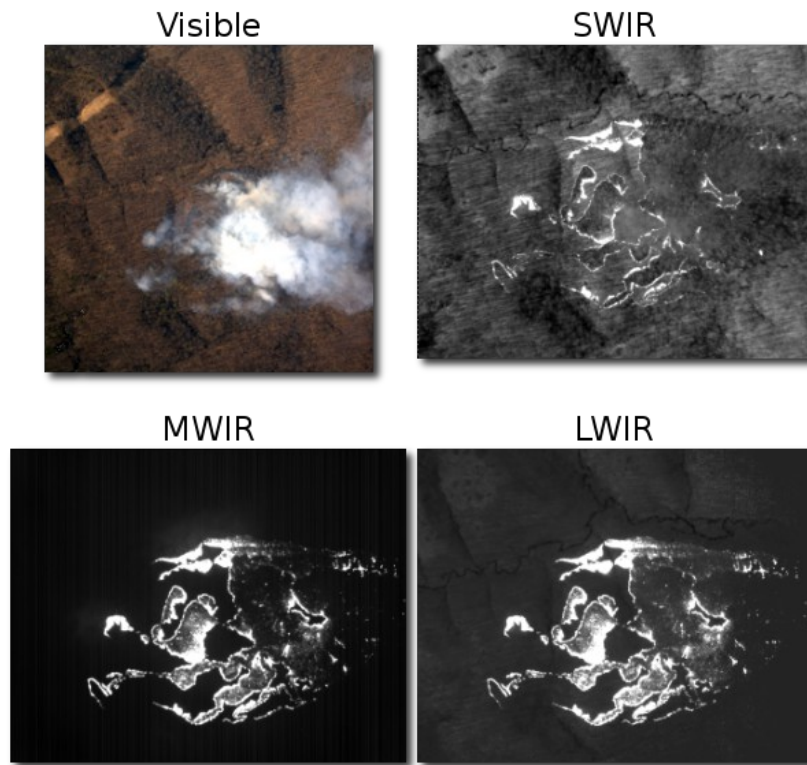


Illustration 2.4.1.2: Forest fire seen by different wavelengths.

However, all that information is useless unless it is possible to measure the burnt areas and the direction of propagation. It is possible to simulate the grow of fire knowing vegetation, wind, slopes, ... but it is impossible to just predict the grow of fires. The UAV analyse code must be able to identity the burned areas by reading the imagery.

Back to the identification of fire, it produces perimeter (curves and polygons), at its turn each point produces a perimeter and so on, burned vegetation will decrease its temperature and extinguish its flame, and will reduce the temperature -meaning that this- But this perimeter follows a pattern of grow expressed by the fire fastest speeds.

Illustration 2.4.1.3: Surface and crown fire.

Illustration 2.4.1.4: Surface fire.

The fire propagates in three ways:

1. surface fire: when the grass is ignited and fire propagates by the surface.
2. corona fire: when the propagation goes from tree to tree.
3. spotting: firebrands, embers, pine cones,... that jump and ignite new areas

They may produce different perimeter although the vegetation. But the eccentricity is determined by the wind speed. The stronger the wind the higher the eccentricity. Slope -or inclination- is another factor. The fire feed itself with the fresh oxygen that exist under the flames while preheating and igniting the new fuel. In the illustration 4.1.6, each point ignites is stretched by the terrain inclination and the wind speed.

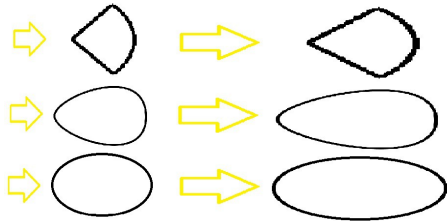


Illustration 2.4.1.6: Different perimeters of different vegetation under different wind speed.

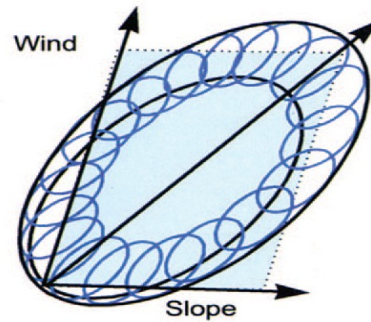


Illustration 2.4.1.5: Perimeter stretched by the wind and the slope (inclination).

The change in the shape is exponential so that's another pattern to recognize a fire raging through the vegetation. Nevertheless, the perimeters are distorted by pathways for fire.

Spotting is another phenomena in forest fires. It is another way to ignite new areas that has never be burned. Wild fires can ignite vegetations which can be far away. The spotting propagation make the detection and tracking of forest fire more difficult; the spotting propagation doesn't follow the perimeter pattern, in other words, it makes more difficult to identify the forest fire.



Illustration 2.4.1.8: Embers from a forest fire.



Illustration 2.4.1.7: Fire crossing the Highway N-II AP-7 (Sample Data Zone).

The firebrands -or any fire particle- are able to easily cross a two-way highway.

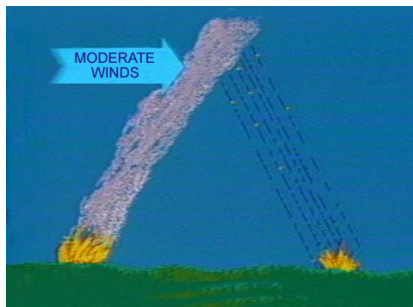


Illustration 2.4.1.10: Firebrand particles under soft wind creating a spot.

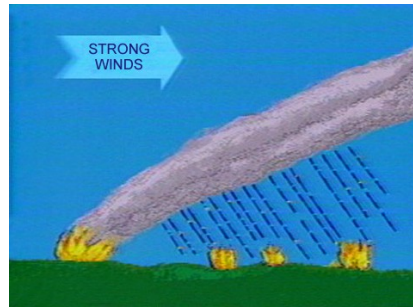


Illustration 2.4.1.9: Firebrand particles under strong wind creating multiple spots.

The objects that cause the spotting are firebrands or embers -as well as pine cones-. The weight, shape and texture of the embers is affected by the wind. Large embers that come from pine cones weigh more than smaller firebrands

2.4.2. Color of fire

In order to identify a fire, this project doesn't only rely on the shape and how it does propagate. The colour of the flame as well as the smoke comprises a range of colour and parameters depending on how and which fuel is provided. The colour of the flame always is comprised between red and yellow. For example, the flame is hardly ever green, blue, pink or cyan. Matlab as well as the opencv library is able to obtain the red, green, blue components as well as the hue, saturation, value (brightness).

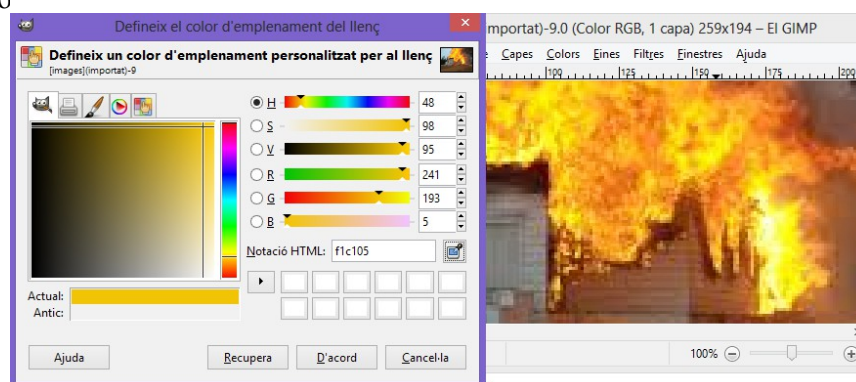


Illustration 2.4.2.1: GIMP application and its palette.

These images can be defined by either the RGB or the HSV meaning Hue, Saturation and Value. There are consistent parameters that define the possibility of presence of fire or smoke. The color of the fire comprises most of –or all- saturation and value (brightness) but it is limited by the hue from red to yellow (0° - 60°).

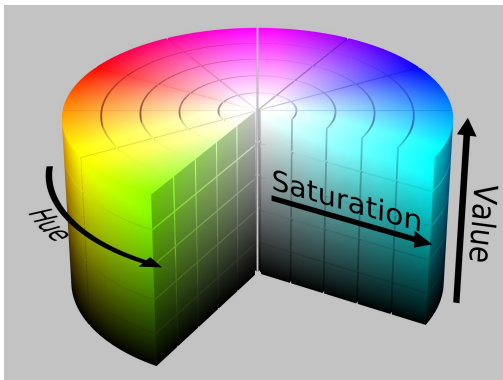


Illustration 2.4.2.3: Relation between hue, value and saturation.

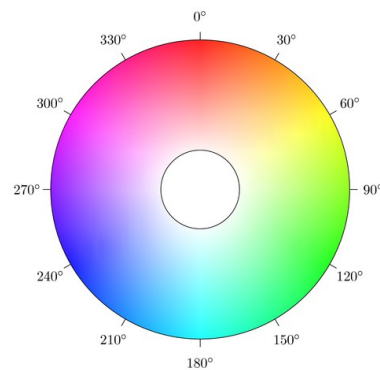


Illustration 2.4.2.2: Hue described by degrees.

Images are usually described by a raster or a grid of pixels that contains RGB (Red, Green, Blue) information³¹ but that implies two inconvenient for the human eye and how to detect ranges of colors especially in case such this one.

³¹ Nevertheless it is useful if some one want to swich or regulated RGB leds of a screen.

In the illustration 2.2.1.12.4.2.4, the flames are being analysed with MATLAB. In order to analyse faster the relation between the RGB (Red-Green-Blue) components, it used the HSV components.

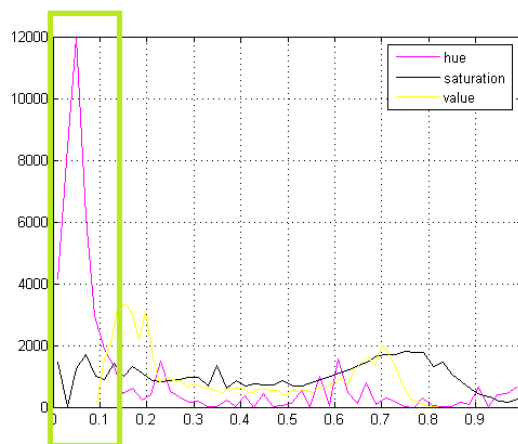


Illustration 2.4.2.4: The hue of the fire dominates.

The pattern that displays the flame is always the same. The hue is from 0° to 60° as it can be seen in the illustration 4.2.4. The drawing angle has been normalized (0° - 360°) Instead of analysing the relation between the components RGB, ranges of hue -or tonalities- are analysed. The yellowish reddish hue is the only component in the flame that doesn't change no matter the flame or the part of the flame.

Smoke detection

The immediate consequence of the fire are heavy columns of smoke. In fact from the point of view of the UAV and because of its elevation most of the indications of fire will be plumes of smoke from high altitude. Visually speaking the smoke is the main symptom of a fire.



Illustration 2.4.2.5: Plumes created by wildfires from high altitude.

The components HSV or RGB that comprises the color of the smokes are harder to find out than the fire color because the fire is not affected by the sun light as it emits and displays its own colors.

The smoke similarly to the fire has a certain constant patterns in the red, green, blue or hue, saturation, value (brightness) components. How is it possible to recognize the color of smoke in a image? Like the patterns that define the fire before, the color of smoke is defined similarly, but instead of a specific hue, it is an specific saturation where no hue prevails over others. The other two components -hue and value- spread across their range.

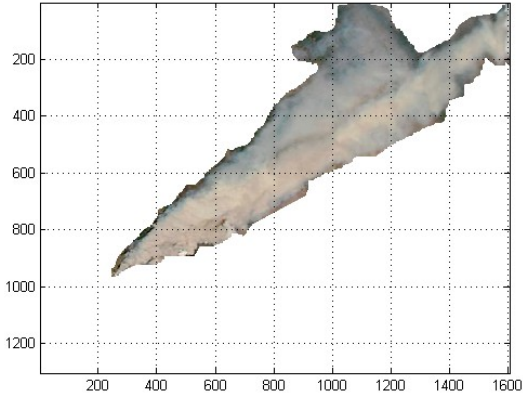


Illustration 2.4.2.6: Smoke from the fire at high altitude.

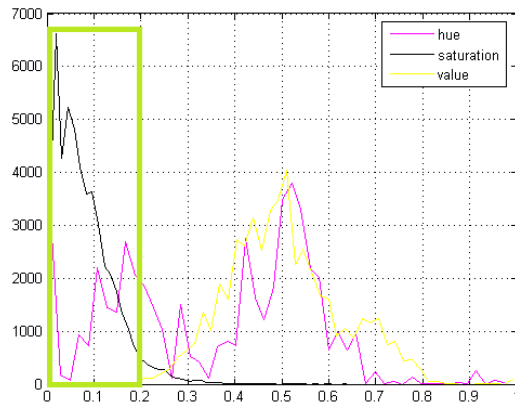


Illustration 2.4.2.7: Pattern that identifies smoke.

The color detection is not enough to detect fire or smoke with certainty. In order to detect fire -not just the color of fire- it is necessary to discard or match the texture. The texture can provide also direction and size of the flame and scale. Or there is another option which is to analyse the contour of the flame or the contour of the smoke and its plume.

2.4.3. UAV cost.

Depending on the company³² and the service, the prices also vary. But this prices are used for low altitude -much less than 10km of elevation-. It is impossible to reach the spatial resolution at 20km. The price are thought for a much lower altitude, but that gives a hint about the price of renting a UAV and sweep an area.

Catuav		
	min	max
Price	3000 € /km ²	6000 € /km ²

³² The company is Catuav. Catuav is an enterprice dedicated to the observation of the Earth with unmanned planes.

Spacial resolution	2m ² /pixel	5cm ² /pixel
--------------------	------------------------	-------------------------

2.5. Manned aircraft-borne analysis.

Airplanes -unlike small drones³³- are able to carry large payloads like radiometers and radars. In that aspects it doesn't differ from the satellite-borne instrumentation. Aircraft-borne sensing has the best of both world. It is near enough to have a better resolution and a plane is able to carry large instruments. The Synthetic Aperture Radar (SAR) in planes makes a special difference.

Although most of the studies on burnt area mapping were based on the use of optical imagery, there are a series of examples in which data from active sensors such as the Synthetic Aperture Radar (SAR) were used. Most of the studies were carried out in boreal forest (Bourgeau-Chavez et al. 1997, 2002, Kasische et al, 1994, French et al. 1999, Siegert and Ruecker, 2000, Menges et al, 2004), but some examples for the Mediterranean area exist (Gimeno and San-Miguel-Ayanz, 2004, Gimeno et al. 2005). Rather than the changes in vegetation condition and structure, the detection of burnt areas from SAR is based on the changes on moisture content in the burnt surface with respect to the unburned areas. Burnt areas tend to have higher moisture content than unburned areas, which reduces the backscatter. Thus, burnt areas appear as dark objects in relation to the surrounding not affected areas.

2.6. Fire lookout towers

Another way to prevent, monitor and fight wildfires are fire lookout tower. It is another option that must be observed. The location and quantity of forest fire lookout tower depend on the terrain, vegetation and even population³⁴ surrounding it. The lookout guard doesn't search for flame or fire but for big well defined plumes of smoke that emanate from the forest fire.

³³ This project considers the maximum payload of a drone 900g.

³⁴ The higher the human population density, the higher the risk of wild fires.

2.6.1. Forest watch towers cost

The summer³⁵ campaign cost between 7000 and 10000 euros for tower in Catalonia. The tower employee earns about 1250 euros a month but the critical factor is its density per area.



Illustration 2.6.1.2: Fire lookout towers in natural park (Parc del Montnegre i el Corredor).



Illustration 2.6.1.1: Geographical location of fire lookout towers.

³⁵ There is just a period of time when the watch tower are active. There rest of the year do not serve that purpose.

There are 18 fire lookout towers in an area³⁶ of 343030 hectares -or 3430km²- of forest in Girona (5905km²). If each installation cost approximately requires 2 lookouts and each one 1250 euros, what would be the cost per area?

$$18 \text{ towers} \cdot \frac{2 \text{ lookout}}{1 \text{ tower}} \cdot \frac{1250 \text{ €}}{1 \text{ month}} = 45000 \text{ €}$$

$$\frac{45000 \text{ €}}{3430 \text{ km}^2} = 13.11 \text{ €/km}^2 \text{ month}$$

36 The designed area is the province of Girona. It has been chosen by the fact that it is where the forest fire takes place. The 5905km² do not actually match with the administrative area which has been parted for fire control but the area is similar in place and size.

However, it is obvious that whole fire lookout towers infrastructure is not just based on the watcher watching the environment in search for fires. There is more people than the ones on the towers who are involved in fire prevention and detection. In the province of Girona there are more than 953 people dedicated to the fire prevention.

$$953 \text{ employees} \cdot \frac{1250 \text{ € min}}{1 \text{ month}} = 1191250 \text{ €}$$

$$\frac{1191250 \text{ €}}{3430 \text{ km}^2} = 347.30 \text{ € / km}^2 \text{ month}$$

This 953 employees include all kinds of works, not only the task of watching the area while searching for smoke plumbs; this new number includes . It is imprecise but that give an idea about how much it might cost to monitor an area by lookout towers.

3. Recognition and analysis of forest fire from one or more drones.

One or more drones will be taking photographs (images), recording video. Such a imagery will be visual and infrared. Regardless if it is done by one or more drones or if it is one or more images, by some means it must be able to assemble all the information or lack of information and draw conclusions.

A number of patterns are defined as indication of wildfire:

- The intensity of the temperature (infrared image).
- The contour of the fire (infrared image).
- The color of the fire (visual image).
- The color of the smoke (visual image).
- The contour of the smoke (visual image).
- The background (visual image).

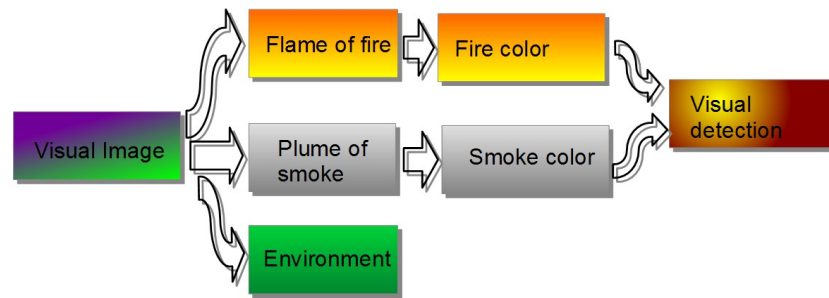


Illustration 3.1: Diagram behind the analysis related to visual imagery.

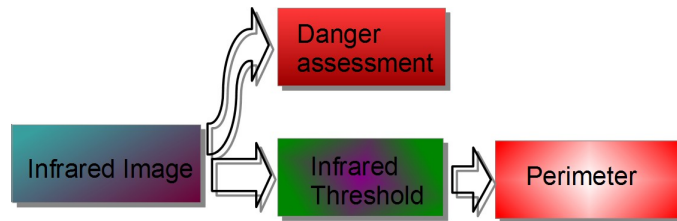


Illustration 3.2: Diagram behind the analysis related to thermal infrared imagery.

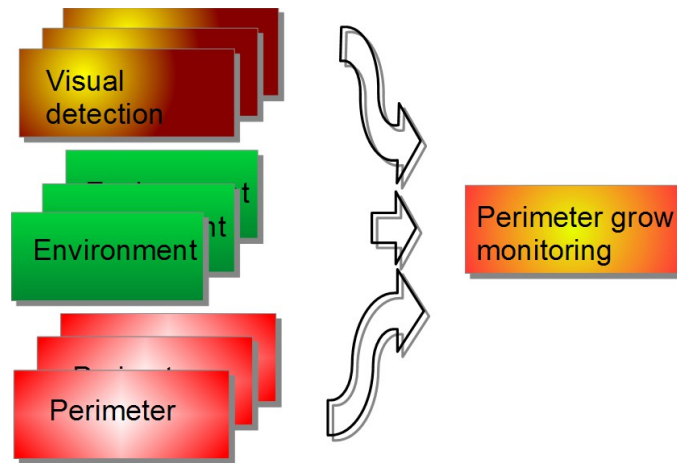


Illustration 3.3: Diagram behind the matching code.

4. Epilogue

4.1. Comparisons and costs

Is there a way to measure the cost versus the benefits comparing the different methods?

4.2. Conclusions

There is an obvious conclusion comparing the SEVIRI data and the images from the thermographic camera. All the described measurements make clear that a radiometer like SEVIRI is unable to detect precise small fires and it is unable to measure of the fire or the flame. Space-borne radiometers from geostationary orbits might be able to detect forest fires but with the current resolution and the “front line” or “perimeter” nature of the forest fire just give the information about whether the fire is burning or not in a 16km² area with the shape of a square.

The comparison is good in order to detail and study each tool, but it doesn't make justice to them. Each instruments obeys to an assigned task that no other is able to perform. Radiometers in geostationary orbits may not be able to measure the burned areas of a forest fire, but they are able to detect dangerous temperature or the presence of a forest fire at a global level. On the other hand radars installed on manned plane -conventional planes - are able to detect burned areas while thermal infrared cameras are able to display the perimeter of flames. Planes and drone cannot operate on a global scale today, so the data provided by the radiometer may prove useful to plane or to warn aircraft-borne or drone-borne and place them.

1. It is possible to extrapolate data from satellite.
2. Faster monitoring.

3. Better prediction.
4. Better measurements
5. Less false positive alerts.
6. Cheaper than permanent Fire Lookout Towers, Manned air-planes and satellite-based remote sensing

4.3. Recommendations for further research

This is the kind of project that

Large amount of imagery is fundamental in order to establish patterns. More images from drone are required especially those which recorded from an elevation between 10km and 20km. These images should include infrared, thermic images while there are many visual -visible band- images, there . And other factor that might be proven useful is the abundance of accurate models of wind, vegetation and terrain; the fire is mainly affected by these three characteristic of an area.

One worry emerge if the UAV are ever used in order to detect monitor a forest fire while planes are being used in order to use remote sensing or throwing water to extinguish the fire.

5. References

[ref.1] Departament d'Agricultura de la Generalitat de Catalunya

<http://agricultura.gencat.cat/ca/ambits/medi-natural/dar_prevencio_incendis_nou/dar_dades_incendis/>

[ref.2] Manygadze, T 2009.

[ref.3] San-Miguel-Ayanz, 2004.

[ref.5] Pili, P 2000.

[ref.6] EUMETSAT (MSG Level 1.5 Image Data Format Description), 2013.

[ref.7] Veronika Zwatz-Meise(2014).

6. Bibliography

- San-Miguel-Ayanz, Jesus; Ravail, Nicholas; Kelha, Vaino; Ollero Anibal. Active Fire Detection for Fire Emergency Management: Potential and Limitations for the Operational Use of Remote Sensing . European Commission DG Joint Research Centre, Institute for Environment and Sustainability. (10 February 2004))
- Zwatz-Meise, Veronika, Introduction into the Solar Channels (Version 1.0. 13 July 2004), EUMETSAT.
- EUMETSAT, MSG Level 1.5 Image Data Format Description, Eumetsat-Allee 1, D-64295 Darmstadt, Germany (4 December 2013)

<<http://www.eumetsat.int/website/wcm/idc/idcplg?>

IdcService=GET_FILE&dDocName=PDF_TEN_05105_MSG_IMG_DATA&RevisionSelectionMethod=LatestReleased&Rendition=Web>

- Jochen Kerkmann (kerkmann@eumetsat.de), D. Rosenfeld (HUI), H.J. Lutz (EUM)J. Prieto (EUM), M. König (EUM) (Contributors), Applications of Meteosat Second Generation (MSG): Meteorological use of the SEVIRI IR 3.9 um channel, EUMETSAT, Eumetsat-Allee 1, D-64295 Darmstadt, Germany (30 June 2004).
- Luis Merino Pablo de Olavide University, Seville, Spain, Fernando Caballero, J. Ramiro Martínez-de-Dios and I. Maza University of Seville, Seville, Spain Anibal Ollero Automatic Forest Fire Monitoring and Measurement using Unmanned Aerial Vehicles University of Seville, Seville, Spain Center for Advanced Aerospace Technologies (CATEC), Seville, Spain.
- Alt Empordà fires of 2012. Wikipedia. Online 16 September 2014 Available at <https://en.wikipedia.org/wiki/Alt_Empord%C3%A0_fires_of_2012>
- Li Cunbin, Zhou Jing, Tang Baoguo and Zhang Ye, Analysis of Forest Fire Spread Trend Surrounding Transmission Line Based on Rothermel Model and Huygens Principle School of Economics and Management, North China Electric Power University, Beijing 102206, (China); Department of Information Technology Shanxi Electric Power Corporation, Taiyuan 030001, (China); Huada Tianyuan (Beijing) Electric Power Technology Co., Ltd., Beijing 102206, (China).

-
- Pili, P., 2000: Calibration of SEVIRI. Proc. 2000 EUMETSAT Meteorological Satellite Data Users' Conf., Bologna, Italy, EUMETSAT EUM P29, 33–39.
 - Shawn P. Urbanski, Wei Min Hao and Steve Baker Chemical Composition of Wildland Fire Emissions (Chapter 4), Developments in Environmental Science, Volume 8.
 - Schmid, J. The SEVIRI Instrument, ESA/ESTEC, Noordwijk, The Netherlands.
 - D.M.A. Aminou, MSG's SEVIRI Instrument, MSG Project, ESA Directorate of Earth Observation, ESTEC, Noordwijk, The Netherlands
 - Philips, Susan. Active Fire Detection using remote sensing based polar-orbiting and geostationary observations: An approach towards near real-time fire monitoring, International Institute for Geo-Information Science and Earth Observation, Enschede, The Netherlands.
 - Anderson, Hal E.; Aids to Determining Fuels Models for Estimating Fire Behavior. Gen. Tech. Rep.INT-122. USDA Forest Service, Intermountain Forest and Range Experiment Station, Ogden, Utah, USA.
 - Mark A. Finney; FARSITE: Fire Area Simulator—Model Development and Evaluation. Rocky Mountain Research Station 324 25th Street, 84401, Ogden, Utah, USA
 - Japan Association of Remote Sensing. Chapter 9 Image Processing: Correction (Remote Sensing Notes) © JARS 1999, Online Available at http://www.jars1974.net/pdf/10_Chapter09.pdf.
 - Ján Kaňák, Overview of the IR channels and their applications, Slovak Hydrometeorological Institute, Jeséniova 17833 15 Bratislava Slovak Republic.